Harold Vance Department of
PETROLEUM ENGINEERING
TEXAS A&M UNIVERSITY

TEXAS A&M PHASE I DESIGN REPORT

Team Member	Tasks	Major
Luis A. Rodriguez	Rig Construction and Drillstring Deflection	Mechanical, Senior
Mohamed Khaled	Team Lead and Drilling Operation	Petroleum, PhD
Muhao Chen	Tensegrity and Controls	Aerospace, PhD
Srivignesh Srinivasan	Drillstring Modeling and Drillstring Deflection	Mechanical, Masters
Thomas Lopez	Drillstring Deflection and Electronics	Interdisciplinary, PhD

Advisors
Dr. Eduardo Gildin
Dr. Sam Noynaert
Dr. Robert Skeleton
Prof. Fred Dupriest

Other Team Members
Ahmed Madi
Alkassoum Toure
Le linh
Rabih El Helou

Acknowledgments

We would like to thank Cameron Geresti, John Maldonado, Enrique Zarate Losoya and Narendra Vishnumolakala for their assistance in preparing for this year's competition. We would also like to thank the organizers and judges for the time they've dedicated to the competition and for the opportunities it presents.

Table of Contents

1. INTRODUCTION 4
2. SAFETY 6
   2.1 Damage to Rig 7
   2.2 Damage to Personnel 8
   2.3 Incident of Fire 8
3. RIG CONSTRUCTION DESIGN 10
   3.1 Mechanical Design of Drilling Rig 10
   3.2 Electrical System 17
4. Drillstring Design 18
   4.1 Drillpipe Design 18
   4.2 Directional Deflection Tool Design 27
5. CONTROL SYSTEM DESIGN AND INSTRUMENTATION 32
   5.1 ROP Optimization Using MSE 32
   5.2 Instrumentation 39
6. DATA ANALYTICS 45
   6.1 Control Architecture, Data Collection and instrumentation 45
   6.2 Optimizing Parameters 46
   6.3 Control Improvements 46
   6.4 Auto-Driller Control system 46
   6.5 Data Visualization 49
7. Project Plan 52
8. Cost Estimates 53
9. References 54

1. INTRODUCTION

The main objective for any driller is to simultaneously drill fast and safe, ensuring quick and accurate execution. Typically, drilling faster means less time spent drilling, which in turn works to reduce costs. At the same time, people are a company's most valuable asset and keeping their well-being intact is of the utmost importance. These objectives can be achieved and maximized with the introduction of automated drilling rigs. Thus, the main objective of any drilling automation process: increase safety by ensuring that well dynamics do not exceed the ones specified by its natural behavior.

Automation in the drilling industry is less advanced as compared to other industries. Failure to adopt new technology in any industry can occur for a variety of reasons. The oil and gas industry, and the drilling sector in particular, have always been slow to take up new technologies due to economics, safety concerns and a low risk appetite. The operator and service company dynamic requires the push for innovation come from the customer. Most operators do not ask for automation and are not willing to pay for it. In addition, a mistrust of automation exists, especially of automation of downhole pressure control. This mistrust is based on the inaccurate assumption that a human can process the data more effectively and make better decisions. Another reason for this slow adoption can be attributed to the fact that drilling activity takes place in extreme working conditions, above ground in inhospitable areas and downhole with high temperature, high pressure (HTHP) formations. Finding control equipment and sensors to handle this environment is difficult. It is also important to note that the drilling process is not standard for all wells as every wellbore construction is unique. Therefore, the modeling of this process cannot be definite, but, instead has to be adaptive. All of these contributing factors make automation in drilling a difficult task. However, with each technological advancement, these limitations are being overcome. It is also no surprise that the recent boom in unconventional reservoirs is adding more motivation for transitioning into automation.

The objective of this year's competition is to drill a wellbore to hit multiple targets at varying vertical depths and X/Y coordinates and to design a closed loop control of the rig based on downhole data. Our main task is to come up with a safe automated drilling system which can achieve drilling optimization within the given constraints. Given constraints include amount of available power, specified drill strings, BHA limitations, directional plan and a specified drill bit. Our automated drilling rig will have a test run to drill 2-ft of block of sandstone and successfully deviate from vertical to reach a specified target.. By optimizing the drilling efficiency in this controlled environment, we believe that what we learn in this research could be applicable in the real drilling operations. The goal is to enable the drilling process to be more productive by managing various risks while keeping a safe operational practice in place. The focus of the project is on maximizing Rate of Penetration (ROP) while also maintaining the required trajectory to drill through the target, thereby optimizing performance.

Directional drilling and closed loop control system are the primary focus for this year's challenge. Mechanical changes to the drillstring and drilling rig will comprise the major changes, with downhole vibration data being implemented into the control algorithm to minimize

vibrations. This report will explain the mechanical and electrical systems of the rig, the sensors, control systems, instrumentation and algorithms used. Data handling, analytics, and visualization are also included, along with cost estimates and a work schedule. Our design plan is based on modifying current rig structure to be meet with Drillbotics requirements and utilize directional drilling concept. We will use a tensegrity structure for rig construction, since it effectively decreases the system weight and improves mobility. Since introducing tensegrity structure in drilling application is completely new, we make contingency plan in case of any obstruction is faced.

2. SAFETY

The safety of personnel involved in any operation should always be the first priority. By removing the physical involvement during the operation, fully automated control drilling system will keep personnel from the hazardous situation. Not only this is advantageous in obvious safety reasons, but will be more economical in today's environment as the liability cost for personnel is very costly.

The automatic drilling system developed in this project operates automatically for most of its tasks. Manual intervention is not required for normal drilling operation. Physical labor is required only during rig setup, transportation and installing machinery. From the statistics obtained from US department of labor, the majority of safety concerns are due to improper handling of machinery or equipment. Safety in the system can be ensured by limiting human intervention during operations as much as possible. This is one of the biggest motivations for implementing automated drilling systems in the field. Figure 1 displays the distribution of injuries at the rig site.

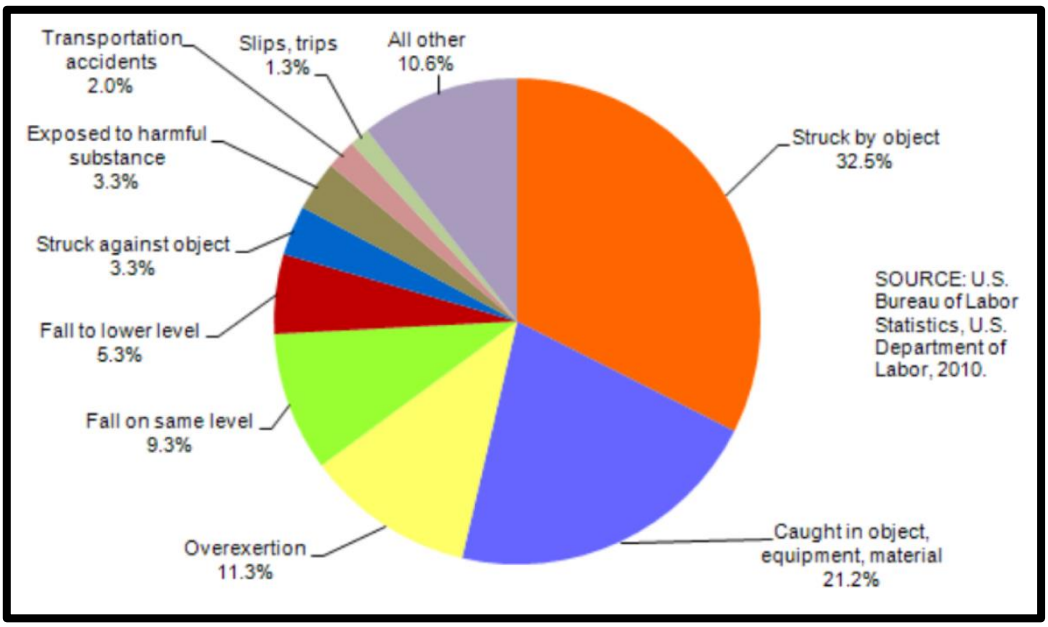

Figure 1: Distribution of accidents and injuries from work in drilling oil and gas wells. Taken from www.oshasafetyconference.org dt. Dec' 2012

Safety (and health) Hazards during operation:

- Chemical Hazards: Dust (cuttings)
- Energy Hazards: Electricity and Mechanical
- Machine Hazards: Rotating parts (motors, pipes), heavy objects
- Other Hazards: Noise

Keeping these hazards in mind, safety operating procedures have been designed to ensure operational safety of plant. Major safety concerns that are relevant to our application (miniature automated drilling) have been identified and listed below. Alarm systems and responses are designed for some critical issues. We have already discussed the alarm systems in section 4.3.1. This list is not comprehensive. Since the system doesn't require a circulation system (for pressure management down-hole) or making connections, many of the safety concerns encountered in actual drilling operations can be ignored here. Now we briefly explain safety concerns and preventive action/ safe operating procedures to avoid each of the concerns.

2.1 Damage to Rig

2.1.1 Motor Failure

We have two motors (one each for drawworks and top drive) in the system. The motors can fail due to overheating (overload), power failure, or for some other unknown reason. An alarm system is designed to detect motor failure and triggers immediate stoppage of drilling operation.

2.1.2 String Buckling

This can occur due to excessive vibrations or torque. The control system (for optimal performance) mitigates dysfunctions. In addition, alerts (warnings) are generated when excessive vibrations are observed in the drill string and the driller can respond if required. As a last line of defense, a shield or netting will be erected around the elevators of the rig to prevent any flying objects from injuring persons.

2.1.3 Bit Damage

Significant bit damage is not possible in this application because the total depth to be drilled is only 2 feet, with WOB and RPM readings well below abnormally high values. The only possibility of bit damage is due to interfacial severity. The algorithm makes sure that RPM is reduced in such situation to avoid extensive bit damage

2.1.4 Software and Communication Errors

Alarm systems are designed to detect sensor or instrumentation failure and trigger stoppage of drilling operation. The operation can be restarted in manual mode or in automatic mode after repairs and maintenance.

2.1.5 Top Drive Containment

A new addition to the rig this year will be the addition of a stopper at the bottom of the rails containing the top drive. This will prevent the top drive from crashing to the rig floor in the case of a drawworks failure. The location is shown in figure 2

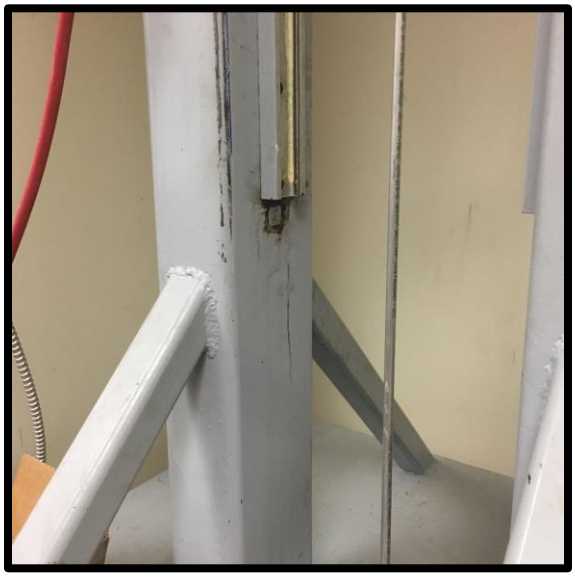

Figure 2: Location for stopper to be welded.

2.2 Damage to Personnel

2.2.1 Struck by Object

The rig consists of a huge mechanical structure (derrick), heavy objects (load), rotating objects (motors and drill pipe) etc. Care must be taken while handling such objects. Wear proper PPE (Personal Protective Equipment) like hand gloves etc. during rig setup. In addition, rig operators should stand behind the plexiglass shield manufactured for use with the rig.

2.2.2 Electric Shock

The power system of rig includes electric power source to motors, pump, sensors communication and data acquisition devices. Wear appropriate PPE while handling equipment. Proper cabling (no loose/open wiring) and grounding should be ensured before switching on the main power supply. Electrical devices should be properly insulated.

2.3 Incident of Fire

2.3.1 Overload of Motor

Tripping system for overload of motor ensures that the equipment does not operate beyond specified capacity. The tripping system is synchronized with the alarm system within the

software and the driller is notified in the event of an incident. In the case of a fire, a fire extinguisher is located nearby.

2.3.2 Overheating of Battery or Electronics

Sensors and other electronics are selected to operate for sufficient time without requirement for cooling. However, if a sensor or any other device fails resulting in loss of communication, the alarm system ensures stoppage of operation. If required, the electronics can be cooled using a fan or compressed air.

2.3.3 Insufficient Cooling

A dedicated circulation system (cool air/ water) is provided for cuttings transport and bit cooling. The circulation is provided at sufficient flow rate throughout the operation to ensure system components do not overheat.

2.3.4 Ignition Sources and Fuel

Since we are not drilling an actual production well we do not have any obvious fuel or ignition source. However, in case of an unexpected incident an emergency shutdown button is provided to suspend power and halt operations. A fire extinguisher is also provided at the rig site.

The above points are shown graphically below in **Fig. 3**.

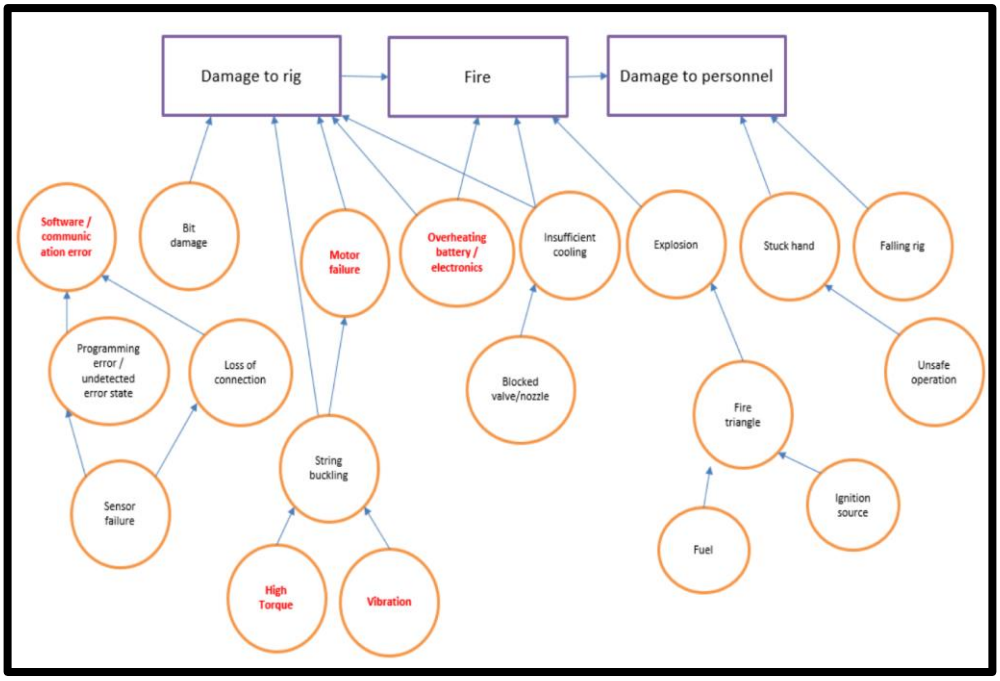

Figure 3: Flowchart summarizing the expected safety hazards

3. RIG CONSTRUCTION DESIGN

3.1. Mechanical Design of Drilling Rig

The rig is required to drill through a 30 x 30 x 60 cm cement block with a 1.5 in. diameter PDC micro-bit that is customized for directional drilling. In previous years, the drilling rig has been one solid piece, but in order to allow for easier transportation methods, the old rig will be adjusted to be able to come apart. The two pillars and four diagonals will be detachable from the base of the table. This year team will be changing the design of the table from previous teams to accommodate for a rig that is much easier to transport. The rig will be situated on a 31" by 28" structure that will allow for the rig to drill the specimen as shown in figure 4. Furthermore, the structure can be extended to 57" to allow space for a 24" workstation and contracted once again to minimize the size of the structure and improve the mobility of the rig when needed (Figure 5). Furthermore, wheels will be attached to the bottom of the four legs to further improve the mobility of the structure since transportation will be needed for this year's competition.

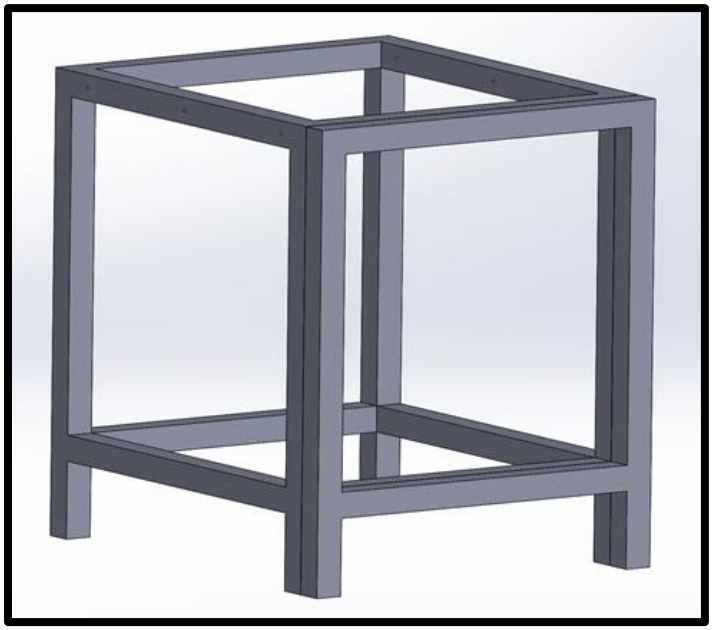

Figure 4: Table in Contracted Positions

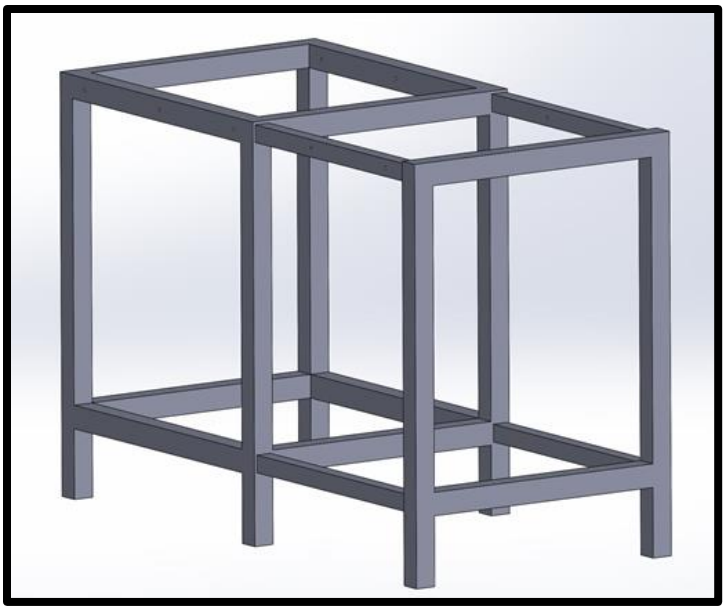

Figure 5: Table in Extended position

This year, the team intends to be able to incorporate a tensegrity structure that will replace the mast with a structure that is lighter and more robust. The concept of tensegrity is experimental which is why there is a back-up rig just in case the structure is inadequate. Nonetheless, the success of this structure would help the concept become known in oil industry and perhaps be adapted in the coming years for real world implementation. This would be beneficial for the drilling industry because the structure will be as robust, if not more, as previous rigs but be significantly lighter and cheaper than traditional rigs and easier in mobility.

Our Current structure is a motor driven drilling assembly supported by two big steel pillars that accommodate for drilling. The new structure will be light and equipped with lightweight metal alloys instead of heavy steel bars and columns. Skelton….et.al demonstrated T-Bar and D-Bar tensegrity systems require much less mass than a single continuum bar under compression. In fact, tensegrity solutions provide the minimal mass for all of the fundamental structural loading conditions in engineering mechanics. Tensegrity is a network of bars and strings, where bars only take compression and strings take tension. All structural members are axially loaded, hence the structural efficiency in strength to mass is very high. There is no material bending, so the static and dynamic model of the structure model is more accurate. This feature increases the precision achievable by feedback control (which relies on the accuracy of the dynamic model). Although we optimize tensegrity structure to handle all expected loads, vibrations and torque; we understand that using tensegrity structure in drilling and extraction is challenging. This why we designed a back-up structure that is based on modifying our current rig structure. Figure 6 & 7 shows our designed tensegrity structure for the mast. The tensegrity structure stands on the grey table composed of two parts: 1. the middle hollow pipe is a DHT (double helix tensegrity) , which is a class-2 tensegrity structure with one set of bars following a clockwise pattern and

another set of bars following an anti-clockwise pattern, a lightweight structure efficient in taking torsion, and 2. The surrounding support is a T2D1 structure (structure efficient in taking compression, Tensegrity System by Skelton 2009). The rig height is 1.2 m tall that stands on a steel which is mounted on the wooden board of the lid. The base of the rig is 1m x 1m wide. The pillars are 2” square columns each made of low alloy steels. This helps in providing a higher strength-to-weight ratio compared to carbon steels and is cheaper than stainless steels. The alloying of steel results in reduction in its tensile strength which is supported by aluminum T-bars of the tensegrity structure. The red bars are the 3003 aluminum alloy bars which are attached to the rings. The rings are equally spaced, attached to the pillars through pin locks. The strings (not shown in the isometric model) will be tightly wound from the rings and hooked to the base plate. This provides the structural stability needed for drilling. The overall mass of the system will be reduced by 17 kg with the implementation of tensegrity.

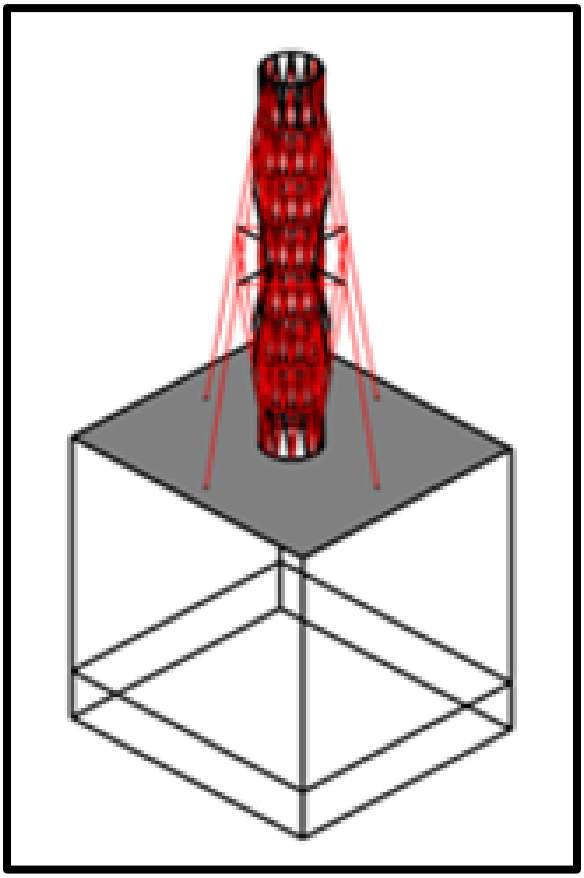

Figure 6: Tensegrity Rig

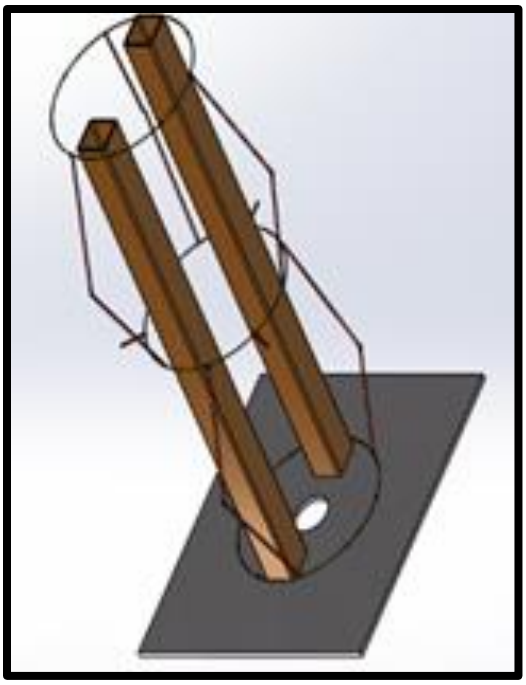

Figure 7: Isometric View

The governing equation of tensegrity statics is given as:

$$NK = W,\ K = C_s^T \hat{\gamma} C_S - C_B^T \hat{\lambda} C_B, \tag{1}$$

Where N is nodal matrix, where each column represents the coordinates of each node, (where tension members connect to compressive or other tension members), □ and □ are force density vectors of strings and bars, is a diagonal matrix of the elements of the vector □. Cs and Cb are connectivity matrices (with 0, -1, and 1 contained in each column) of strings and bars, and W is external force on the nodes. The atmospheric pressure and the centrifugal forces from the rotation provide all compressive forces needed to stabilize the inflated structure. Yielding is mode of failure for the strings. Using the same material for all the strings, the minimum mass M required for the cable network is:

$$M = \frac{\rho_s}{\sigma_s} \sum_{i=1}^{\alpha} \gamma_i ||s_i||^2 + \sum_{j=1}^{\beta} max(\frac{\rho_b}{\sigma_b} \lambda_j ||b_j||^2, 2\rho_b \lambda_j^{\frac{1}{2}} (\frac{||b_j||^5}{\pi E_b})^{\frac{1}{2}}), \tag{2}$$

Where \rho_s and \sigma_s are density and yield strength of strings and where \rho_b, \sigma_b, and E_b are density, yield strength, and Young's Modulus of bars. Material used for strings:

Spectra (Ultra High Molecular Weight Polyethylene, UHMWPE). Aluminum: E_b = 60e09 Pa, rho_b = 2700 kg/m3, sigma_b = 110e06 Pa. UHMWPE Density: E_s = 120e09 Pa, rho_s = 970 kg/m3, sigma_s = 2.7e09 Pa.

It is also important to know the dynamic behavior of the structure. A compact matrix form for the full system dynamics including string masses can be written as [7]:

$$\ddot{N}\mathrm{M_s} + \mathrm{NK_s} = \mathrm{W} + \Omega\mathrm{P^T},$$
$$K_s = \left[C_s^T \hat{\gamma} C_{sb} - C_{nb}^T C_b^T \hat{\lambda} C_b \; C_s^T \hat{\gamma} C_{ss}\right],$$
$$\hat{\lambda} = -\hat{J}\hat{l}^{-2}\left[\dot{B}^T \dot{B}\right] - \frac{1}{2}\hat{l}^{-2}\left[B^T(W + \Omega P^T - S\,\hat{\gamma}\,C_s)C_{bn}^T C_b^T\right]. \quad (3)$$

where Cnb, Cb, Csb, Csb, Css represent different connectivity matrices for bar to string, string to string and bar to bar nodes, is the Lagrange multiplier, P is the constraints matrix.

Based on the non-linear class-K tensegrity dynamics equations, a non-linear control law is shown in figure 8. The control variables (force densities in strings) appears linearly in the non-linear dynamics.

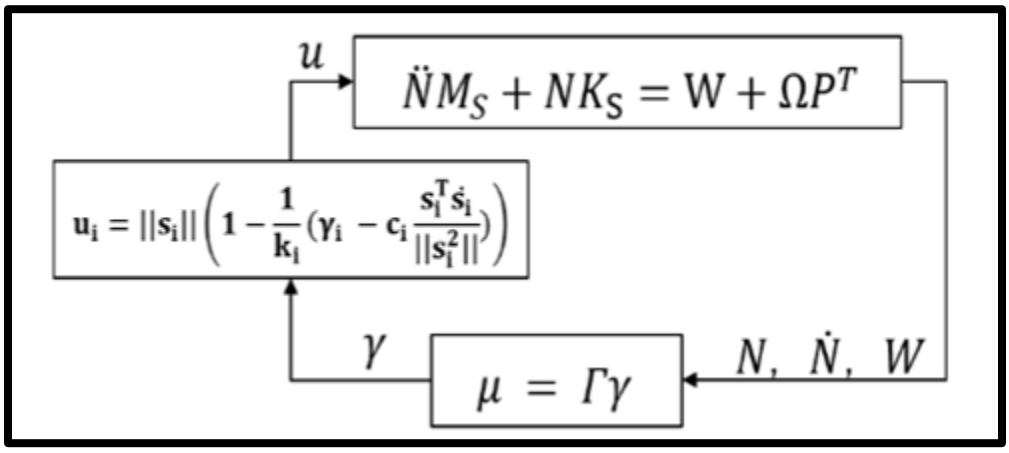

Figure 8: Close loop system, where u is control input and ui is the rest length of the string

Moreover, the team has modified the 2019 TAMU Drilling Rig to be collapsible to be used as a back-up if the tensegrity structure were to fail during testing in the spring semester. The backup rig will have four 45 degree supports as well as four L supports screwed into the two pillars to provide added support for the drilling rig. . The rig that is demonstrated in the figure 9 will be modified to be collapsible. It will consist of two steel pillars that contains drilling instrumentation between them. The overall height with the rigs situated on the table will be no taller than 80”. There is a designated section on the table where the rig will be situated and

directly underneath will be a section where the drilling specimen can be placed securely to be drilled into. The figure below represents the table with the new modified rig situated on it.

Figure 9: Solidworks Model of Back-up Drilling Rig

3.1.1 Drilling Rig

The important structural parts of the rig are as follows:

a) Base and steel support pipes.
b) Drawworks motor with a pulley mechanism to control the top drives position.
c) Locking casters used to support the steel pipes and to provide the rig mobility. Separate plates to anchor the locking casters to the ground will be used for rig stability.
d) A slip ring to convert the rotating wires in the pipe into stationary output wires, thus allowing for wired downhole telemetry

3.1.2 Drilling Technique

We decided to use conventional rotary drilling for this rig. We elected to use a top drive system in our rig design. Although the time saving with the top drive will not be realized in our simulation as only one stand of drill strings will be used, it will aid us in delivering sufficient weight to the bit. The Kelly drive system was considered as the Kelly bushing would act as a centralizer which would help in stabilizing drill string. However, we decided that strategic

placement of the bell nipple would provide us with the same stability. Besides that, power system is also limited to the electrical power from the local grid not to exceed 25 hp.

The important structural parts of the top drive in this system are listed as follows:

a) The top drive motor is rated at 2.5 HP with a maximum rotary speed of 2000 rpm with minimal torque forces.
b) The swivel is placed between the top drive motor and the drill string.
c) Guide rails and clamps will serve as the elevator for the top drive, allowing the system to drill a vertical well, and have an estimated load limit of 114 lbf.

3.1.3 Power System

Constraints have been placed on the power system we can use for our drilling rig. Normally, diesel engines would be used to generate power on the rig site. This power is utilized throughout the rig, mainly in the mud circulation, hoisting, and rotary systems. In our competition the power system is also limited to the electrical power from the local grid not to exceed 25 hp. In our case, most power will be utilized in the rotary system to maximize the rotary speed of the drill strings. Since we are going to be drilling in atmospheric conditions, minimal power is required to run the mud circulation system. Similarly, minimal power is needed in the hoisting system as we do not have to lift heavy drilling strings.

3.1.4 Hoisting System

The hoisting system serves many functions in the drilling operation. It includes the derrick, drawworks, traveling/crown block, and drilling lines. The main function is to raise and lower the drill strings during connections, trips, and drilling. In our hoisting design, making connections and multiple trips is not required.

3.1.5 Drilling Fluid Circulation System

There are many functions of drilling fluid system. An effective drilling fluid system is needed to ensure well stability, remove rock cuttings, and lubricate/cool the drill bit. The system includes mud pumps, various mud mixing equipment, mud pits, shale shakers, etc. In our design, the primary concern was to effectively cool the bit and remove drill cuttings from the system. Other functions are ignored as we are drilling a 2 ft. concrete block in the atmospheric condition. Air will be pumped up to remove rock cutting out of the hole. Air will be pumped to enter the drill string through a swivel. Then, air will travel through the drill string down to the bit and then carry cutting up through the annulus. A t-pipe segment will be situated at the borehole to further stabilize and centralize the drillstring and to allow for the cuttings to be collected outside the hole in a small tank. A closed loop fluid circulation system will be utilized with an air valve serving as the source, and a shop vacuum serving as the filtration system. A high flow rate vacuum is used to ensure cuttings removal is not a performance limiter.

As a BOP (blowout preventer) stack is not required in our rig design, we decided to place a bell nipple between the rig floor and the rock sample. This bell nipple consists of a rubber gasket, flange, and flow outline. This bell nipple will allow sufficient transportation of cuttings from the annular space to the flow line while providing a sufficient seal.

Another important consideration regarding the drilling fluid circulation system is the design of the swivel, placed between the top drive and the drill pipes. The swivel is required to allow simultaneous drilling fluid circulation and drilling string rotation.

3.2 Electrical System

Two DC Motor drivers capable of handling analog control signals are used to provide power to both the top drive and drawworks motors. An H-Bridge is used to reverse the direction of the electrical system used in conjunction with an Arduino as a codifier and the DAQ as the source of the control signal the project is depicted as follows. Figure 10 depicts the motor control schematic.

Water pumps, motors, and sensors use 12 VDC which is supplied by a switch-mode power AC/DC converter rated for a maximum of 10A of current draw.

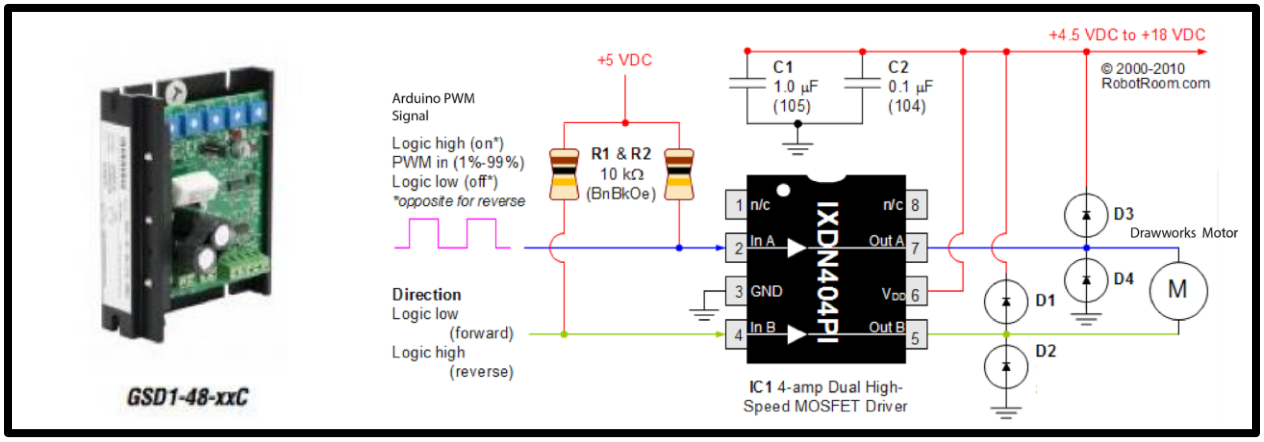

Figure 10: Motor control system drive and control schematic

4. DRILLSTRING DESIGN

4.1. Drillpipe Design

Drill string will transmit the torque from the top drive to the drill bit as shown in figure 11. The deflection of drill string causes torsion and bending stress whereas the vibrations due to drilling cause axial and tangential stress. The combined von-mises stress will decide the torque transmission to the drill bit. Previous tests have shown that the drillstring can withstand more than 75 lbs of WOB that the previous team had limited the control system. This is for a vertical well though, as different WOBs will be tested at different inclinations. Recent testing has also shown the maximum allowable torque before failure to be about 30 lb-in, beyond which failure of the drill pipe connectors generally occurs. Because the drill pipe connectors are the limiting factor in terms of our maximum deliverable torque, different types of connectors and methods of connection are currently being investigated. The guide rails will have the breaks to hold the top drive when it is not in use.

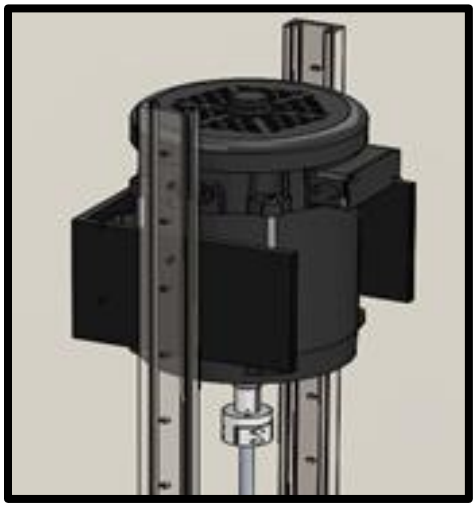

Figure 11: Driver Assembly

Two options were considered for drill string material: Stainless steel and Aluminum alloy. The buckling of stainless steel is 4 times more difficult than that if aluminum because of its compressive strength. The fatigue strength of stainless steel is twice as much as aluminum alloy. This ensures that the drill string can last for more number of cycles. The drill string will be manufactured out of stainless steel because of the material's high fatigue limit and compressive strength. Furthermore, the material's high compressive strength allows for the drill string to resist buckling caused by the Weight-

on-Bit. Making drill pipe connections and installing casing strings is not required and therefore not considered in the design.

It is important to understand the forces experienced by drill string to predict its failure. The most important mechanical properties of tubing are burst strength, fatigue resistance and compressive/ tensile strength. These properties are necessary to determine the strength of the pipe and to design a casing string. In this section, we will consider the mechanics of various failure modes and calculate the safety factor for each failure mode.

Design of drill string mainly involves, the thickness of the tube and the material composition. The drill bit for this year's competition will be a micro bit of 1.5" diameter and 2" length instead of 1.25" diameter that was used last time. This allows for larger drill string or thicker shell. Instead of 3/8" OD that was used last year, we are thinking of increasing it. To start the testing, we will use 0.5" OD drill string. The length of string is maintained at 36". 3 different thickness (0.016", 0.035" and 0.049") and 3 different materials (Al 6061-T6, SS 316L, SS 304L) were considered for design calculations. Further assumptions, if any, will be clarified as we proceed with calculations.

Symbols used:

OD: Outer Diameter

ID: Inner diameter

t: wall thickness

L: Length of tube

Ys: Yield Strength

A: Cross sectional area of the tube

I: Second moment of inertia

E: Modulus of elasticity

PR: Poisson's Ratio

Rg: Radius of gyration

Rc: Radius of Curvature

M: Moment

Pbl: Burst pressure limit

pi: internal pressure

po: External pressure

St: Tangential stress (hoop stress)

Sr: Radial Stress

Sa: Axial Stress

Svme: Triaxial Equivalent von-mises stress

Sst: Maximum Shear Strength

Sb: Bending Stress

Tmax: Maximum Torque

Fa: Axial Load

Fb: Buckling load

Fcr: Critical buckling force

S_{buck}: Critical buckling stress

4.1.1. Burst:

Bursting occurs when the internal pressure of a pipe exceeds the maximum allowable pressure limit. The bursting pressure limit can be calculated based on the dimensions of the tube and the yield strength of the material. The burst pressure, also called as minimum internal yield pressure of the pipe body is determined by the internal yield pressure formula found in API Bull. 5C3, Formulas and Calculations for Casing, Tubing, Drillpipe, and Line Pipe Properties.

$$Pbl = (0.875 * 2 * Ys * t) / OD \quad (4)$$

The Barlow equation for tubular burst is commonly used in the industry to calculate the burst pressure of a pipe. The ratio of OD to thickness of the tube, called as slenderness ratio, gives an idea of the nature of tube. If OD/t >>1, which is the case with the model that we have now, a thin wall assumption can be made. The Barlow equation give a reasonable result for thin walled tubes and an overly conservative result for thick walled tubes. Additionally, API burst pressure rating, which is based on Barlow's equation, includes a 0.875 reduction factor to take uncertainties about pipe thickness into account.

The burst pressure limit gives an indication of the internal pressure when the tangential stress at the inner wall of the tube becomes equal to yield strength. Table 1 showing the limit for each thickness and different material composition is given below.

Table 1: burst pressure limit calculation

	S.No	t (in)	OD (in)	ID (in)	L (in)	Slenderness Ratio (OD/t)	Yield Strength (ksi)	Burst pressure limit (ksi)
Aluminum 6061-T6	1	0.016	0.5	0.484	36	31.25	39	2.18
	2	0.035	0.5	0.465	36	14.29	39	4.78
	3	0.049	0.5	0.451	36	10.20	39	6.69
Stainless Steel 316L	4	0.016	0.5	0.484	36	31.25	42	2.35
	5	0.035	0.5	0.465	36	14.29	42	5.15
	6	0.049	0.5	0.451	36	10.20	42	7.20
Stainless Steel 304L	7	0.016	0.5	0.484	36	31.25	32	1.79
	8	0.035	0.5	0.465	36	14.29	32	3.92
	9	0.049	0.5	0.451	36	10.20	32	5.49

Thicker pipe is better to withstand bursting as it can be seen from the table above. For the same thickness, SS316L provides more strength to withstand internal pressure compared to Al 6061 or SS304L.

The internal pressure should never exceed the limit mentioned above. But for all practical purposes, the internal pressure should be only half the Pbl, considering a safety factor of 2. This will ensure that the combined pressure also will be lesser than Pbl. So for future calculation, the operating internal pressure is taken as half of the burst limit, which is a reasonable assumption based on last year's data. The external pressure will be mich lesser compared to the internal pressure. To simplify the analytical calculations, external pressure is taken as zero, even though it will not be exactly zero (but close to zero w.r.t internal pressure).

$$pi = Pbl/2; \qquad po = 0 \tag{5}$$

4.1.2. Twist:

Twisting occurs when the drill string is subjected to pure shear stress. Beyond a certain limiting torque, the shear stress will exceed the ultimate shear strength of the material. The maximum torque which the drill string can withstand is given by equation:

$$Tmax = \pi/16 * Sst * (OD2 - ID2) (OD+ID) \tag{6}$$

Sst is calculated using the yield strength and the individual stress components (St, Sr, Sa).

4.1.3. Von-Mises Stress:

The overall stress is due to the axial loading (weight on bit) and the internal pressure. The WOB contributes only to the axial stress component. The internal pressure influences all 3 stress components. The external pressure is assumed to be zero, which in turn does not contribute to any stress. The stresses due to the internal pressure is given by the following equations:

$$St = ID2\ pi * (1 + OD2/D2) / (OD2 - ID2) \quad (7)$$

$$Sr = ID2\ pi * (1 - OD2/D2) / (OD2 - ID2) \quad (8)$$

$$Sa = ID2\ pi / (OD2 - ID2) \quad (9)$$

It can be observed from the equations (7) to (9) that the maximum value of stress will occur at the inner wall (when D = ID) and minimum value will occur at the external wall of the tube (i.e, when D = OD). The triaxial equivalent von misses stress can be calculated, which will give an indication of the strength of the material.

Table 2: Internal pressure and other input variables for stress calculation

	S.No	t (in)	OD (in)	ID (in)	Yield Str. (ksi)	Internal pressure (ksi)
Aluminum 6061-T6	1	0.016	0.5	0.484	39	1.092
	2	0.035	0.5	0.465	39	2.389
	3	0.049	0.5	0.451	39	3.344
Stainless Steel 316L	4	0.016	0.5	0.484	42	1.176
	5	0.035	0.5	0.465	42	2.573
	6	0.049	0.5	0.451	42	3.602
Stainless Steel 304L	7	0.016	0.5	0.484	32	0.896
	8	0.035	0.5	0.465	32	1.960
	9	0.049	0.5	0.451	32	2.744

Table 3: Von Mises Stress calculations

	S.No	t (in)	Tangential Stress (ksi)	Radial Stress (ksi)	Axial Stress (ksi)	Equivalent VMS (ksi)	Safety factor
Aluminum 6061-T6	1	0.016	33.588	-1.092	16.248	30.157	1.293
	2	0.035	32.974	-2.389	15.293	30.750	1.268
	3	0.049	32.539	-3.344	14.597	31.203	1.250
Stainless Steel 316L	4	0.016	36.172	-1.176	17.498	32.476	1.293
	5	0.035	35.510	-2.573	16.469	33.116	1.268
	6	0.049	35.042	-3.602	15.720	33.603	1.250
Stainless Steel 304L	7	0.016	27.559	-0.896	13.332	24.744	1.293
	8	0.035	27.056	-1.960	12.548	25.231	1.268
	9	0.049	26.699	-2.744	11.977	25.602	1.250

The triaxial equivalent von-mises stress for all models are approximately the same. It confirms that the material will not fail due to static loading. Fatigue strength of these material are considered to further distinguish the behavior of materials. When cyclic stresses (S-N curve) is taken into consideration, stainless steel 316L has better durability compared to aluminum 6061. Thus, going with a stainless steel tubing is a better option for longer cycles.

4.1.4. Bending Stress:

When the drill string changes its direction to drill horizontally, an axial stress is induced by bending the tube. The bending stress varies as a function of distance from the neutral axis. The neutral axis for a perfectly hollow cylindrical tube will be at its center. So the maximum banding stress will be at the extreme end of the tube. One end will experience maximum tension, whereas the opposite end will experience maximum compression. Assuming the materials remain in the elastic region, the maximum bending stress will be at the outer wall (OD/2) and the value is given by the equation:

$$Sb = M * OD / (2*I) \quad (10)$$

$$M = E\ I / Rc \quad (11)$$

To drill directionally for about 18", the minimum radius of curvature will be 18". Four different Rc values were taken considering the deviation that will be required to achieve in this competition. The Rc values are 48", 36", 24", 18". As expected the bending stress increases as radius of curvature is reduced. Best values are achieved when the Rc value is 48". But increasing the radius of curvature has a disadvantage that maximum deviation may not be achieved within 2 ft of the rock formation. The maximum bending stress and comparison with yield strength is given in the following table.

Table 4: Variation of bending stress with thickness

	S.No	t (in)	OD (in)	Yield Str. (ksi)	E (ksi)	I (in^4)	Rc (in)	M (x1000) (lb.in)	Bending stress (ksi)
Aluminum 6061-T6	1	0.016	0.5	39	9990	2.99E-03	48	0.623	3.25E-03
	2	0.035	0.5	39	9990	6.18E-03	48	1.287	6.70E-03
	3	0.049	0.5	39	9990	8.30E-03	48	1.727	8.99E-03
Stainless Steel 316L	4	0.016	0.5	42	28000	2.99E-03	48	1.746	9.10E-03
	5	0.035	0.5	42	28000	6.18E-03	48	3.607	1.88E-02
	6	0.049	0.5	42	28000	8.30E-03	48	4.840	2.52E-02
Stainless Steel 304L	7	0.016	0.5	32	28000	2.99E-03	48	1.746	9.10E-03
	8	0.035	0.5	32	28000	6.18E-03	48	3.607	1.88E-02
	9	0.049	0.5	32	28000	8.30E-03	48	4.840	2.52E-02

In the above table, the radius of curvature was assumed to be 48". If we change the radius of curvature (shorten the radius, as it will be required in the competition) keeping the thickness constant, a different trend emerges. Aluminum tubing has a better elastic response to bending compared to stainless steel. Using stainless steel will also work but

as the table shows, it will be increasing difficult to bend. The table below shows the bending stresses for 0.016" thick walled tubes for each radius of curvature and all 3 materials. 3 times higher force is required to bend a SS316L tube compared to Al 6061 tube, as data suggests. This aspect will be studied in detail using the RSS prototype to check if RSS can generate the required force to bend the stainless steel tubing. If the hydraulic piston pressure can be increased within the geometric constraints of the model, then enough pressure can be attained to bend the drill string and a stainless steel tubing will be used. The prototype for RSS is being made and the experimental results will suggest the way forward.

Table 5 : Variation of bending stress with radius of curvature

	S.No	Yield Str. (ksi)	E (ksi)	R (in)	M (x1000) (lb.in)	Bending stress (ksi)	Bending factor (in %)
Al 6061 T6	1	39	9990	48	0.6231236	3.25E-03	120.17
	2	39	9990	36	0.8308315	5.77E-03	67.59
	3	39	9990	24	1.2462473	1.30E-02	30.04
	4	39	9990	18	1.661663	2.31E-02	16.90
SS 316L	5	42	28000	48	1.7464927	9.10E-03	46.17
	6	42	28000	36	2.3286569	1.62E-02	25.97
	7	42	28000	24	3.4929854	3.64E-02	11.54
	8	42	28000	18	4.6573138	6.47E-02	6.49
SS 304L	9	32	28000	48	1.7464927	9.10E-03	35.18
	10	32	28000	36	2.3286569	1.62E-02	19.79
	11	32	28000	24	3.4929854	3.64E-02	8.79
	12	32	28000	18	4.6573138	6.47E-02	4.95

4.1.5. Buckling:

When a tube (fixed at both ends) is subjected to compressive loading, it bends and breaks at the cross section at a stress much lesser than the compressive strength of the material. This phenomenon is called buckling. The critical buckling load for regular cross sections can be calculated based on the geometry of the setup. In our case, one end attached to the motor is considered fixed and the extreme end attached to the drill bit is allowed to twist (pin joint). For this type of configuration, the critical buckling load is given by the Euler equation:

$$Fcr = 8\ \pi 2\ E\ I\ /\ L2 \qquad (12)$$

This does not take in to account the thickness of the tube and hence the values do not exactly match the experimental results. For thin walled tubes (OD/t > 15), Johnson Formula gives a better estimate of the critical buckling stress, given by:

$$Sbuck = Ys (1 – 0.71 L / (2\pi Rg E)) \quad (13)$$

$$Rg = (I/A)1/2 \quad (14)$$

This critical buckling stress is a better estimate to compare the actual buckling stresses in the drill string as opposed to the yield strength.

The buckling load consists of the axial load (due to weight on bit and bending force) and the load due to internal pressure. This can be calculated by the equation:

$$Fb = Fa + pi Ai + po Ao \quad (15)$$

Table 6: Buckling safety factor w.r.t thickness of material (for WOB = 1000 lb)

	S.No	t (in)	Yield Str. (ksi)	Internal pressure (ksi)	Buckling limit (ksi)	Buckling force (lb)	Buckling stress (ksi)	Buckling safety factor
Aluminum 6061-T6	1	0.016	39	1.092	38.968	1200.911	6.116	6.371
	2	0.035	39	2.389	38.967	1405.664	7.159	5.443
	3	0.049	39	3.344	38.967	1534.247	7.814	4.987
Stainless Steel 316L	4	0.016	42	1.176	41.988	1216.365	6.195	6.778
	5	0.035	42	2.573	41.987	1436.869	7.318	5.738
	6	0.049	42	3.602	41.987	1575.342	8.023	5.233
Stainless Steel 304L	7	0.016	32	0.896	31.991	1164.850	5.933	5.392
	8	0.035	32	1.960	31.990	1332.853	6.788	4.713
	9	0.049	32	2.744	31.990	1438.356	7.325	4.367

The buckling force increases with increase in wall thickness as the internal pressure increase is more than the increase in the cross sectional area of the tube. This results in higher stress on the tube and a comparatively lower safety factor. The weight on bit is assumed to be 1000 lb. The variation of buckling stress with WOB force is also computed to understand the relation. Based on previous recorded data, the maximum WOB did not exceed 1500 lb. To compute the maximum buckling stress, WOB must be increased to maximum. So weights of 500, 1000, 1500 and 2000 lb were considered and the safety factor was calculated for each model. The result is shown in table below.

Table 7: Buckling safety factor with variation of WOB

	S.No	Yield Str. (ksi)	Internal pressure (ksi)	Buckling limit (ksi)	Axial load (lb)	Buckling force (lb)	Buckling stress (ksi)	Buckling safety factor
Al 6061 T6	1	39	1.092	38.968	500	700.911	3.570	10.916
	2	39	1.092	38.968	1000	1200.911	6.116	6.371
	3	39	1.092	38.968	1500	1700.911	8.663	4.498
	4	39	1.092	38.968	2000	2200.911	11.209	3.476
SS 316L	5	42	1.176	41.988	500	716.365	3.648	11.508
	6	42	1.176	41.988	1000	1216.365	6.195	6.778
	7	42	1.176	41.988	1500	1716.365	8.741	4.803
	8	42	1.176	41.988	2000	2216.365	11.288	3.720
SS 304L	9	32	0.896	31.991	500	664.850	3.386	9.448
	10	32	0.896	31.991	1000	1164.850	5.933	5.392
	11	32	0.896	31.991	1500	1664.850	8.479	3.773
	12	32	0.896	31.991	2000	2164.850	11.025	2.902

The analytical solution suggests that 316L grade stainless steel will be better for drillstring because of its high strength. All the safety factors are measured with reference to the yield strength of the materials. The same can be done taking fatigue strength of the material as reference and the results follow the same pattern. Although stainless steel 316L is the stronger material among the three, the cost of Al tubing is much lesser and even Al 6061-T6 grade tube can be used to operate the drill string without failure. The selection of the thickness of the material is not as straightforward as the material grade selection. A thin wall is better for bending whereas thick wall is better to prevent bursting. Thin wall is preferred for buckling limit and on the other hand thick walled tube has higher resistance to twist off. So, we will test our prototypes with stainless steel 316L tubing of 0.5” OD and 0.035” wall thickness.

4.2. Directional Deflection Tool Design

One of the objectives of this year's competition is to drill a wellbore to hit multiple targets at varying vertical depths and X/Y coordinates. This why we will build an in house rotary steerable assembly (RSS) as shown in figure 12 to deviate the wellbore. RSS will be connected to the drillstring. The rotary steerable system consists of two universal joints for power transmission through the drill axis. The universal joints are connected to each other through connecting shafts. The connecting shaft closest to the drill bit will be housed by the down-hole sensor assembly which would contain sensors for acquiring rotation angle (encoder), accelerometers, gyroscope and temperature sensor. The assembly would also contain a flex sensor at each the universal joint to give feedback on the bend angle at the universal joint. The pistons would also contain a linear position sensor to track the piston actuation. The assembly contains four pistons. As the pistons are actuated, the steering collar is pushed to the desired configuration and thereby actuating the drill bit itself to the angle required with respect to the drill hole axis. The four medium pressure fittings would be connected to their respective hoses that would bring the hydraulic fluid required for piston actuation. Pressure inside each of the piston assembly will be controlled top

side. With this assembly, we would be able to attain directional drilling through the formation to create the desired hole trajectories to extract water more effectively.

On the other hand, the casing will be manufactured out of aluminum since its ductility will help the drill string to deflect at different inclinations. Furthermore, the aluminum casing will be situated with roller bearings inside to ensure that the drill string is centralized throughout the drilling operation. The following illustration in figure 13 shows where the roller bearings will be situated:

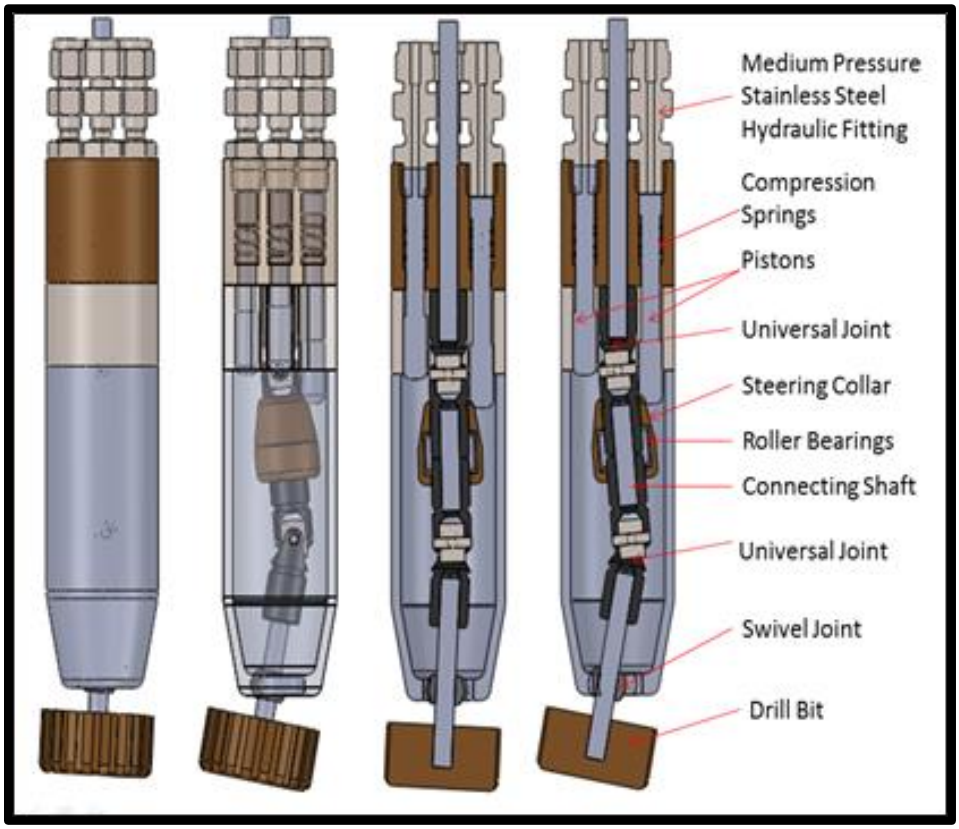

Figure 12: Rotary Assembly

Figure 13: Location of Roller Bearings in Drillstring

The casing allows for different instrumentations to be situated between the non-rotating casing and rotating drill string so that sensors are able to accurately detect the location of the drill string.

Downhole sensors will be situated before and after the deflection section according to their specific purpose. For example, the gyroscope will be situated after the deflection section so that accurate angles can be tracked to ensure that the drill string is deflecting in the desired direction. Figure 14 illustrates an example of how the instruments will be fixed to the casing:

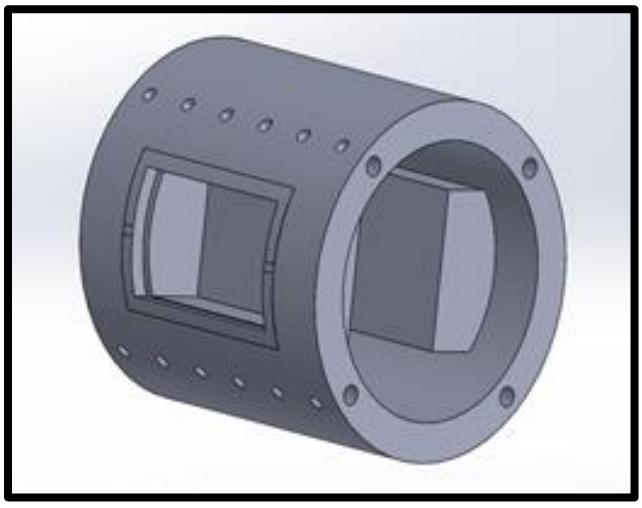

Figure 14: Cross-sectional view of Instrumentation on Casing

The bit will be redesigned to be 1.5” diameter and 2” in length with low axial aggressiveness and high side aggressiveness. We are planning to use a two-blade cutter for the drill bit based on experimental tests done by our previous teams that show its superior drilling efficiency as shown in figure 15

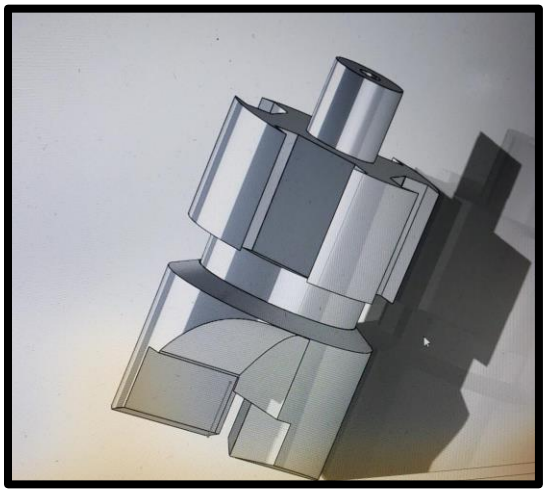

Fig 15:- Drill Bit

Rotary Steering system is one technique used in the industry to assist directional drilling. A much simpler technique that has been in use since 1960s is the use of positive displacement motor in the bore. This technique is also planned as back up to the RSS design, in case of RSS implementation faces any challenges. Positive displacement motors are directly attached to a drive which is connected to the drillbit. Some minor modifications in the PDM technique can help in steerable motor assemblies as opposed to vertical drilling. A small-scale model of the PDM is designed that can be attached with the existing drillstring and bit assembly.

To design a PDM, it is important to understand the mechanics of its working. It is based on the Moineau principle. The principle developed by Rene Moineau, the theory states that a helical rotor with one or more lobes will rotate eccentrically when the stator contains more lobes than the rotor. The flow of the fluid transmits power allowing the assembly to rotate and turn the bit. The PDM, also called as mud motor uses the Moineau pump principle to convert hydraulic energy to mechanical energy: a rotor/stator pair converts the hydraulic energy of the pressurized circulating fluid to mechanical may be categorized with respect to the number of lobes and the effective stages. The speed and torque of a power section is linked directly to the number of lobes on the rotor and stator. The greater the number of lobes, the greater the torque and the lower the rotary speed. Typical rotor/stator configurations can vary from 1:2 to 9:10 lobe. The power section should be matched to the bit and the formation being drilled for best performance. Both rotor and stator lobe profiles are similar, with the steel rotor having one less lobe than the elastomeric stator. The rotor and stator lobes are helical in nature, with one stage equating to the linear distance of a full “wrap” of the stator helix.

The directional steering of the drill bit is made possible using a component called, bent housing. The important thing to consider while designing the bent housing is the angle of inclination and twist that the drill bit can make in a specified distance. This is characterized by dogleg severity (DLS). The build rate is calculated using a three-point curvature calculation, given by the equation:

$$Rb = 200\,\Theta / (L1 + L2) \tag{16}$$

Where Rb is build rate, Θ is angle of bend, L1 and L2 are distances from the bit to the bend and bend to the motor stabilizer, respectively. For a DLS of 15 degree per 100 ft, the bend angle is approximately 4 degrees. The bent housing with a 4 degrees bend angle is supported by a single universal joint to assist the transition or change in direction.

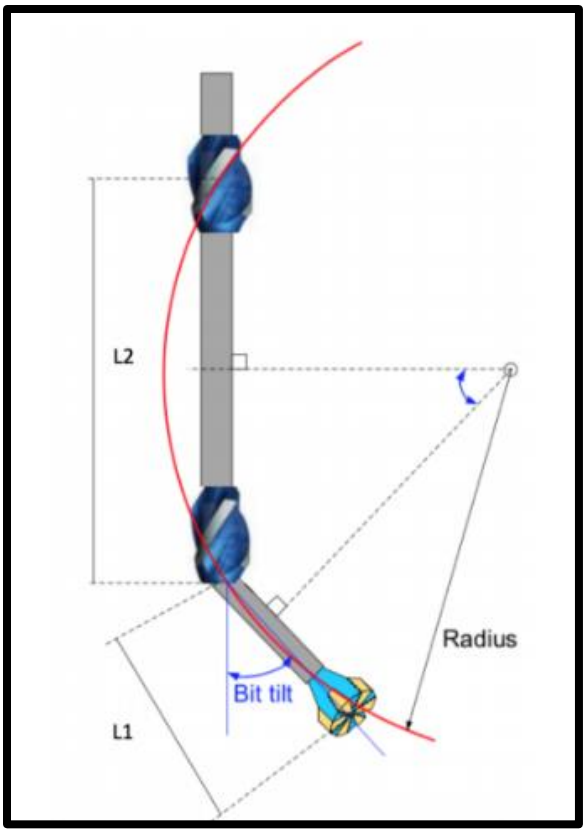

Figure 16: An illustration of the DLS in a bent-housing assembly (not an original design)

The hydraulic bearing accommodates the drive shaft that will make the drill bit rotate and the bearing assembly. The bearing assembly usually consists of multiple thrust-bearing cartridges, radial bearings, a flow restrictor, and a drive shaft. The thrust bearings support the down thrust of the rotor, the hydraulic down thrust from bit pressure loss, and the reactive upward thrust from the applied WOB.

5. CONTROL SYSTEM DESIGN AND INSTRUMENTATION

5.1 ROP Optimization Using MSE

Fundamentally, drilling automation is the control of drilling processes via computer instead of humans. Therefore, designing control system for the processes is key in automation. For automatic control of the rig, we have designed a few control systems in this application. The most important one is the control system for ROP optimization and directional control.

The Rate of Penetration (ROP) depends on several factors such as WOB (which creates rock indentation – higher WOB implies deeper indentation), motor RPM (which creates cutting length on the rock – higher RPM implies more sliding distance), bit aggressiveness and rock strength among other non-linear effects. For a given bit type and a given formation, ROP can be optimized using WOB and RPM. The relationship of some of these factors are illustrated in figure 17

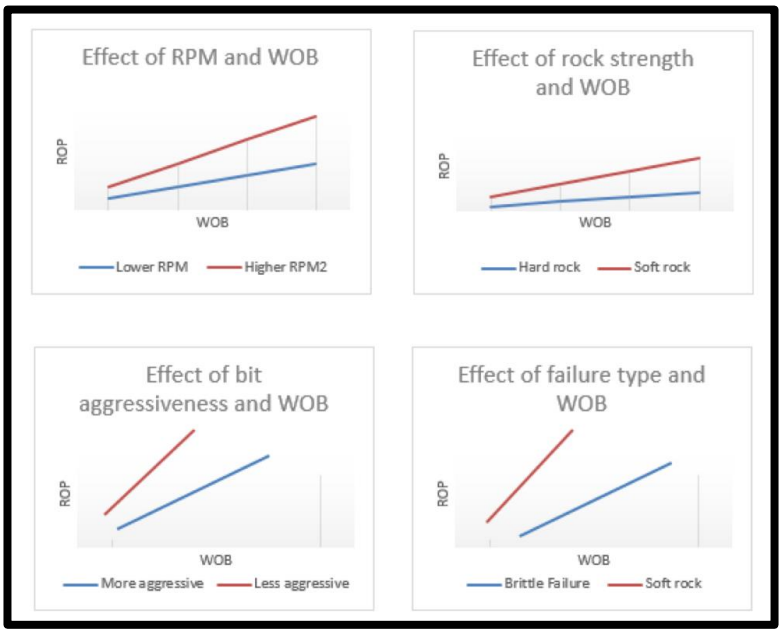

Figure 17: Relationship of ROP with various parameters

The algorithm is developed based on the concept of Mechanical Specific Energy (MSE). The Mechanical Specific Energy (MSE) concept has been widely used to quantify the efficiency of the energy used to remove the volume of rocks in drilling operation. This concept was first suggested in 1965 by Teale in “The Concept of Specific Energy in Rock Drilling”. However, it

did not get much attention as it should in the academic research until Exxon Mobile implemented MSE surveillance throughout the company worldwide in the early 2000. Since then, there have been several laboratory scale drilling experiments and industry application based on the MSE concept, and many successful cases have been reported. MSE can be mathematically expressed with total energy input and total rock volume removed as shown below.

According to Teale, there is a distinct correlation between the MSE and the strength of the rock. Not only is there is a positive correlation, but the MSE should equal to the rock strength if the drilling system is one hundred percent efficient in just cutting the rock volume.

$$MSE = \frac{Energy\ Input}{Volume\ of\ Rock\ Drilled} \tag{17}$$

Expanding the above equation, the MSE equation becomes:

$$\text{MSE} = \frac{(Energy\ Input\ from\ Vertical) + (Energy\ Input\ from\ Rotation)}{Rock\ Volume\ Removed} \tag{18}$$

And it can be expanded with WOB, RPM, Torque, ROP, and bit-diameter to produce the below equation.

$$\text{MSE} = \frac{(4 \times WOB)}{Bit\ Dia^2 \times \pi} + \frac{(480 \times Torque \times RPM)}{Bit\ Dia^2 \times ROP} \tag{19}$$

Such that:

MSE = Mechanical Specific Energy, psi.

WOB = Weight-On-Bit, lbs.

Bit Dia = Bit Diameter, inches.

Torque = Torque from rotation, ft.-lbs.

RPM = Rotation per Minute

ROP = Rate of Penetration, ft./hr.

The importance of the MSE concept does not only lay in its physical meaning but the application of the surveillance program to optimize rock cutting efficiency. Simply put, ROP can be optimized by minimizing the MSE, and we can get this done by varying the three variables in

real time through the surveillance program or having a modification to the existing engineering design to remove limiting factors prohibiting lower MSE realization.

The control algorithm is based on the above formula. Using the parameters WOB & RPM, the system is designed to minimize MSE and thus improve ROP. The parameters are adjusted as long as the MSE value decreases or remains constant. The ROP should increase proportionately to increase in WOB and RPM. If the increase is not proportionate, it is an indication that the bit is performing inefficiently and that a dysfunction is present in the system, as shown in Figure 18

.

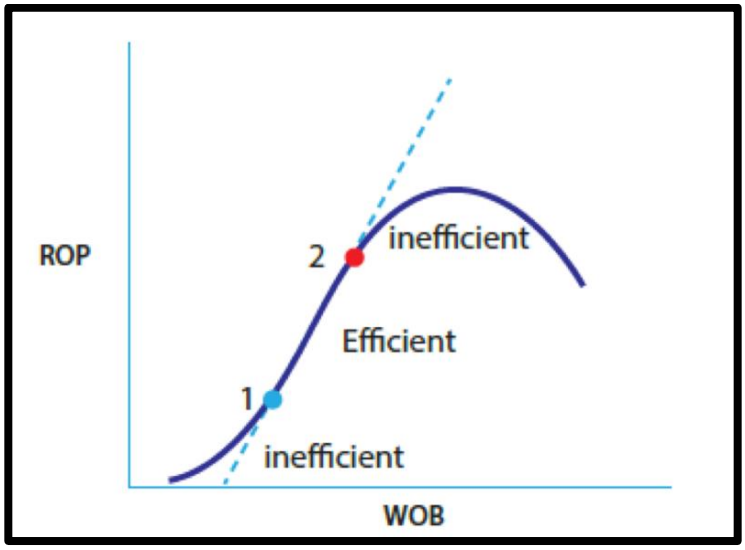

Figure 18: The bit is considered performing efficiently if ROP increase is proportionate to WOB

Beyond Point 2 (the founder point), the bit is performing inefficiently.

In our application, we have the control algorithm, based on the surveillance program, to automatically change variables to minimize the MSE in real time by eliminating possible dysfunctions. There are several types of dysfunctions that can occur down-hole, to the drill-string or to the drill-bit namely

1. Bit balling
2. Bottom-hole balling
3. Interfacial severity
4. Whirl (Lateral Vibrations)
5. Stick-slip (Torsional Vibrations)
6. Axial Vibrations

The type of dysfunction can be diagnosed using MSE and corrective action corresponding to the dysfunction is taken to optimize performance this is shown in a ROP v WOB chart in Figure 19. Each of the dysfunctions is briefly explained below. For the miniature drilling system, some of the dysfunctions may not be significant and can be ignored in the control algorithm at this point of time. The applicability of the dysfunction to our current application are also described below.

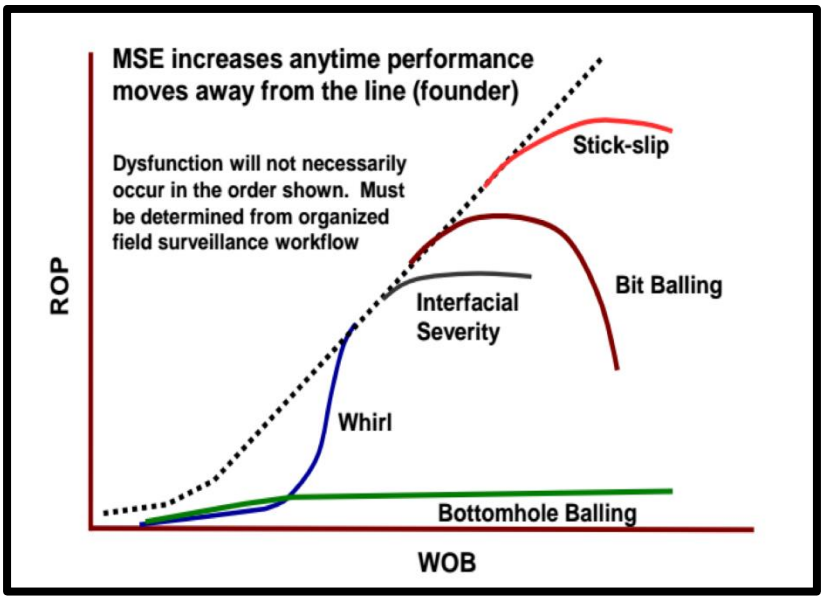

Figure 19: The most common dysfunctions encountered and the response of ROP to drilling parameters like WOB is shown here.

5.1.1 Bit balling

It is the accumulation of material on the face of the cutting structure that interferes with depth of cut when weight is applied. As material is compacted, it builds compressive strength and is able to carry some of the bit load, which reduces the depth of cut (DOC). Balling then occurs and adversely effects ROP. MSE tells us the severity of the effect on DOC, torque and ROP. It should be noted that balling is not simply material stuck to the bit. It must be material on the cutter itself that is strong enough to interfere with depth of cut.

Response

Increase pump (flow) rate to use all horsepower. Reduce WOB to below the founder's point to reduce DOC and cut a thinner ribbon to mitigate balling. This results in loss of ROP which can be compensated by increasing RPM.

Applicability

Balling is rare (usually associated with shales) and is observed under high hydrostatic heads. Given the size of rock sample (2 ft. TVD) and BHA (1.5 inch dia PDC drill bit), the chances of bit balling are minimal and are ignored in the performance optimization algorithm. Even if there was a situation of bit balling, since the maximum WOB is approximately no more than 80 lbf

(due to drill pipe strength), it is safe to assume that this low WOB is below the founder point, the weight on bit is not reduced and RPM is increased. Additionally, testing done in the previous years has shown no evidence of bit balling occurring.

5.1.2 Bottom-hole balling

This usually occurs when the hydrostatic head is very high and in deep impermeable rock (shale). Bottom-hole balling is observed when the rock cuttings accumulate and form a layer at the bottom. BHB results in a very high MSE value and ROP becomes unresponsive to WOB.

Response

Since ROP is unresponsive to WOB, all that can be done is to maximize hydraulics (Increase flow rate) and increase motor RPM.

Applicability

It is almost impossible to have bottom-hole balling in our application because the hydrostatic head cannot be large for a 2 ft. deep hole. Also, it is more common with insert bits and is rare with PDCs. Additionally, testing done in the previous years has shown no evidence of bottom hole balling occurring.

5.1.3 Interfacial severity

When a hard material is encountered in the formation, bit force is concentrated on the bit cutter in contact with the hard material causing bit damage. In uniform rock, the load per area on the cutter face equals the rock compressive strength. But if a formation includes very high strength material, high point loading occurs at the contact points with the cutter.

Response

Reduce WOB to limit bit damage. Operate at moderate RPM values.

Applicability

Interfacial severity failure is not common. When it is encountered it is usually only for short intervals in an entire well (unless you are drilling horizontally in the zone). Also, usually only in wells with general rock strengths above 10-20 ksi. Therefore, this situation is ignored in our optimization algorithm for the 2 ft. rock sample drilling operation. Though there were layers of hard formation, it is optimum to drill off the layer at the existing operating parameters as the layer would not be more than a few inches. But one corrective action that is included in the algorithm is to reduce RPM to prevent bit damage. Additionally, testing done in the previous years has shown no evidence of interfacial severity damage occurring.

5.1.4 Whirl

When the bit is rotated using the drill string, any imbalance tends to cause the BHA to flex and develop a sine wave resulting in lateral vibrations. The wave may rotate with the string in a jump rope action, or it may oscillate across the hole. This lateral movement of the string off center is referred to as whirl.

Response

The magnitude of the wave has to be reduced on order to mitigate lateral vibrations and improve ROP, bit life and borehole quality. Primary response to whirl is to increase WOB to increase the DOC to suppress the bit tilt due to the sine wave. RPM must be changed to ensure that the hole is not resonating.

Applicability

Whirl can occur when there is imbalance in BHA (worse at resonant RPM). Mitigating this dysfunction is important in our application because the clearance is small (drill pipe is 1'' dia and drill bit is 1.5'' dia) and small lateral vibrations can affect borehole quality significantly. But, the drill pipe provided is very stiff (1'' OD and 7/16'' ID) which makes it difficult for whirl to propagate. The algorithm is designed in such a way that when whirl is encountered, WOB is increased to its maximum design limit and ROP is increased slowly as long as MSE is not increasing. Based on testing done in previous years, bit whirl is likely to occur. Figure 20 depicts the result of whirl in rock samples drilled last year.

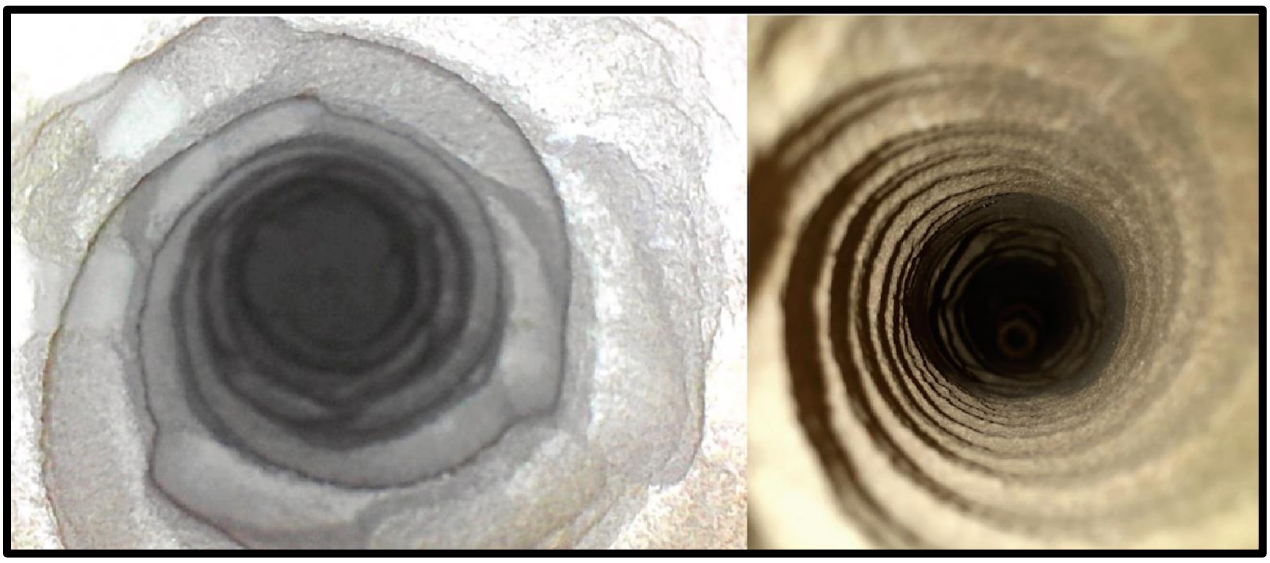

Figure 20: The resulting pattern left over from a hole drilled under severe whirl

5.1.5 Stick-slip

The torque due to motor rotating the drill pipe generates bit torque and drag causing the drill string to twist and turn. Stick slip is a resonant-period torsional oscillation in the drill string. While the RPM at the surface is constant, the bit is speeding up and slowing down as the string winds and unwinds. If the amplitude is small, this is called an "oscillation". If the swing in speed is so great the bit comes to a full stop during its backward motion, it is called "full stick-slip".

Response

The shape of the torque curve at the surface will be symmetric if we are experiencing only oscillations. It will be non-symmetric if the bit is fully stopping for any period of time. Increasing WOB causes an increase in bit torque which drives higher torque oscillations. Effect on MSE is usually subtle up to the point that the accelerations cause full stick-slip. RPM is increased to keep ROP high.

Applicability

This type of dysfunction usually is dominant when the drill string is long. The chances are high when a small diameter drill pipe is used. In previous years, this was not a problem with vertical holes due to the high stiffness. With trajectory though, there could possibly be a higher chance of it occurring so we will prepare for it.

The previously described points are summarized in Table 8**.** Figure 21 shows a clean hole with no dysfunctions which is the objective for this project.

Table 8: Overview of the most common dysfunctions, likelihood of occurrence, and the remedy technique

Type of Dysfunction	WOB	RPM	Concern
Whirl	↑	↓	Yes
Stick-Slip	↓	↑	Yes
Bit Balling	↓	↑	No
Bottom-hole balling	-	↑	No
Interfacial Severity	↓	-	No

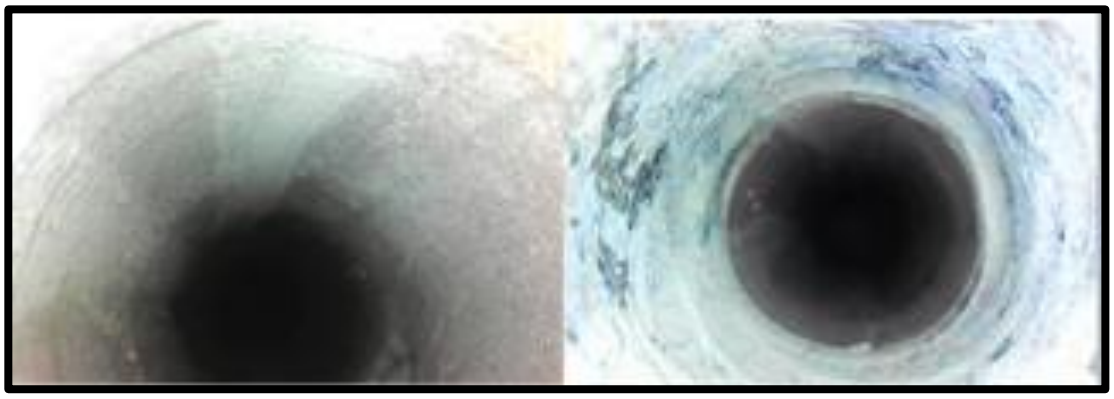

Figure 21: A clean hole drilled without any dysfunctions.

5.2 Instrumentation

A control system model is designed based on the concepts described in the previous section. To implement the control system in the actual application, data is to be transferred from plant to the control system and vice-versa. Measurements are made at the plant using sensors (or transducers) and are given as input to the control system (in computer). Outputs based on the control algorithm are given to the plant using actuators. An interface is required for communication and data transmission between the plant (hardware) and control system (software). These three topics Sensors, Actuators, and Data Acquisition are addressed in this section.

5.2.1 Sensors

We have identified some key parameters that have to be measured in real-time to ensure a much robust performance as well as plant safety. Using downhole sensors specifically designed for this small diameter are out of commercial available solutions options. Thus, we focused our efforts in determining a much better way of not only acquiring data but analyze it in real-time in our control loop. Thus, the biggest improvement over last year's development is going to happen within the software and optimization scope to a much greater level.

Weight-On-Bit (WOB)

WOB is a major parameter to not only monitor but control. To do so, we will utilize an S-Beam load cell, shown in figure 22, to measure tension in the cable of the hoisting system (drawworks) and relate it to the weight being applied on the bit.

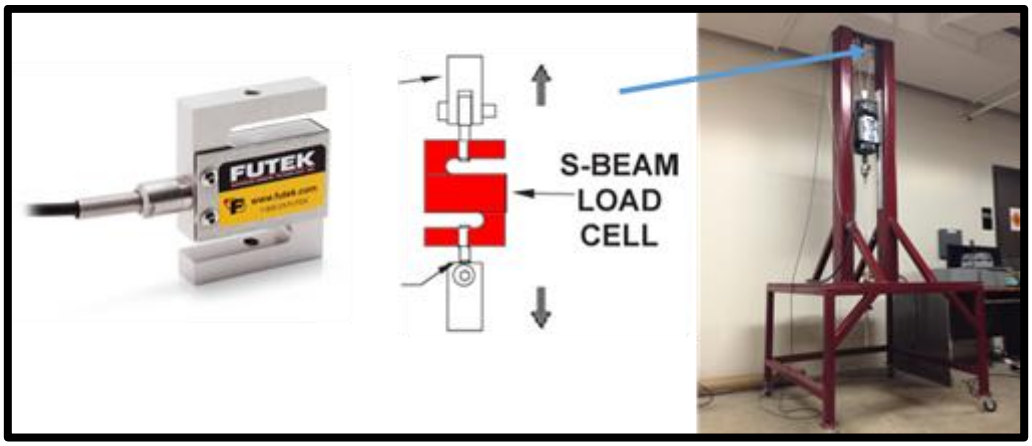

Figure 22: WOB sensor used and its location on the rig

Revolutions-Per-Minute

RPM is measured with an Optical Tachometer, shown in figure 23**,** which consists of an infrared diode coupled with a light-dependent resistor. Any analog variation in voltage is transformed to a frequency from which we can infer the RPM at which the motor is operating. Motor speed and voltage are controlled using Pulse Width Modulation (PWM), which controls the DC motor driver's input, in turn controlling the amount of voltage supplied to the motor.

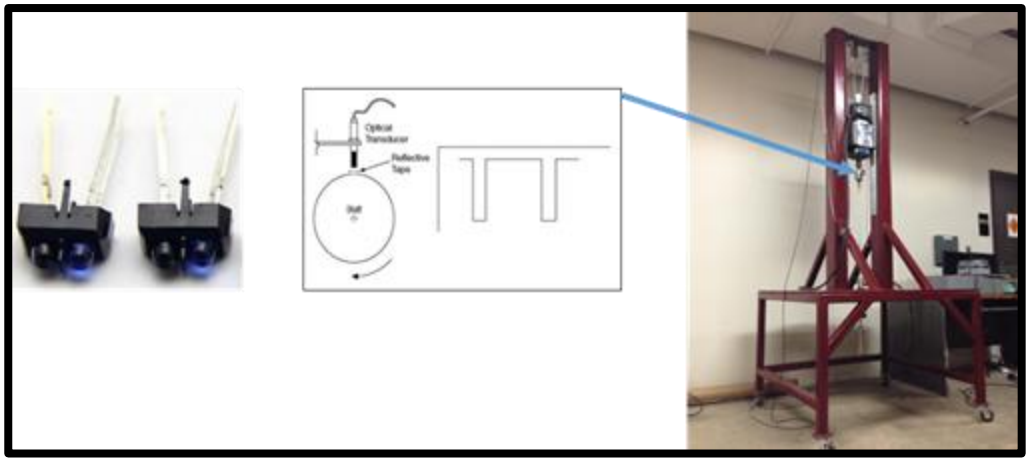

Figure 23: RPM Sensors and Location

Torque

Torque measurements are obtained using two methods, an AcuAMP DC current sensors is going to be purchased. Giving us high performance and reliable sensing of current from which we can calculate the amount of torque acting on our drill string. Power losses in gearbox and couplings are assumed negligible. Proper calibration ensures accurate measurements.

Measuring a voltage in any system is a “passive” activity as it can be done easily at any point in the system without affecting the system performance. However, current measurement is “intrusive” as it demands insertion of some type of sensor which introduces a risk of affecting system performance.

Current measuring is vital in our task. By knowing the current and the voltage, power of DC motor could be introduced and the control scheme will be based on this measuring data. As it has been told above, a “non- intrusive” or an “indirectly” method should be employed, which is going to be applied in our work- “Hall Effect” current sensor.

The Hall Effect, shown in Figure 24**,** is the production of a voltage difference (the Hall voltage) across an electrical conductor, transverse to an electric current in the conductor and a magnetic field perpendicular to the current. It was discovered by Edwin Hall in 1879.

As we all know, the magnetic field will be generated by the current flow. By amp’s law and ohm’s law the variation of current will lead to the magnetic flux density difference in the air gap, which will generate the voltage correspondingly. By the OP Amplifier circuit, we can get the sensor output, which is also the current measure data.

A direct torque measurement will also be coupled and compared with the indirect method. The direct measurement involves inserting a torque sensor in line with the rotating shaft. The direct torque sensor utilizes a built-in strain gauge to identify the real-time torque applied across the sensor. Due to the short nature of the string, it will be assumed that there are minimal Torque

losses between the bit and the sensor. As such, the Torque measured across the sensor will be an accurate representation of the torque across the bit.

In this work, the AcuAMP DCT100-42 series of DC current sensors is employed as the indirect sensor and a Futek TRS300 is employed as the direct inline sensor and are shown in figure 25**.** The direct sensor has a maximum rated current of 50A. The direct sensor has a maximum torque of 10Nm (88.51 in lbs). Both these capacities are enough to meet our requirements while allowing sufficient data resolution.

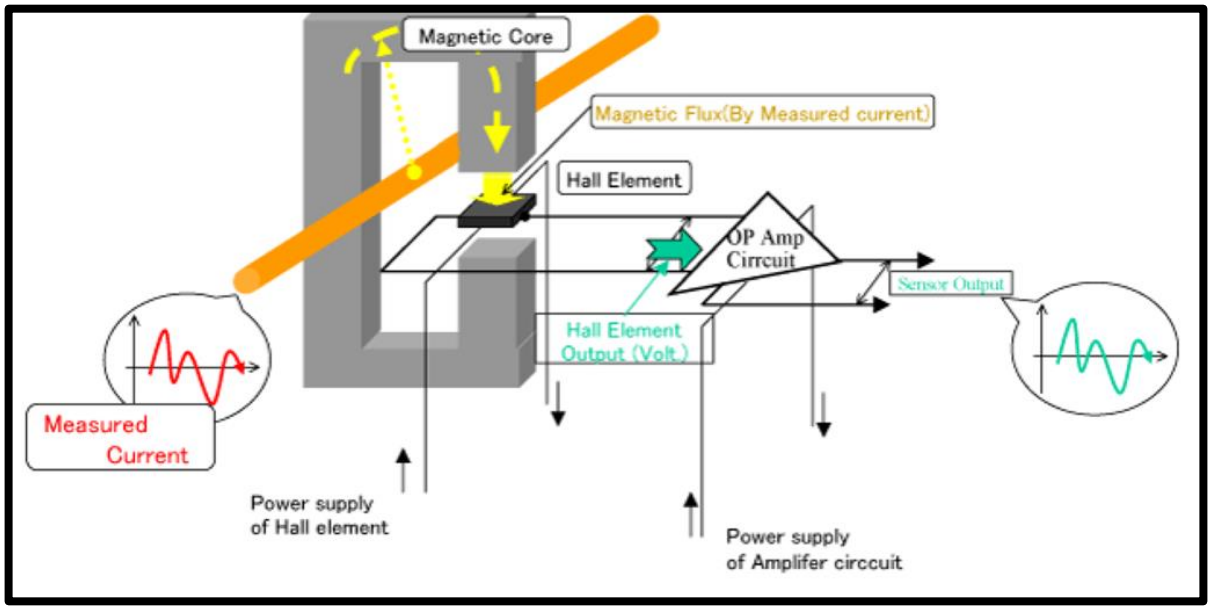

Figure 24: The Hall Effect

Figure 25: Torque sensors to be used. Indirect sensor left. Direct sensor right.

Rate of Penetration (ROP)

ROP will be calculated using linear regression. Since the well planned is a vertical well, we will use a Linear Variable Differential Transformer, shown in figure 26**,** to measure displacement. A

change to be implemented this year is altering the datum to the rig floor. Previously, the depth was measured from the top of the rock sample.

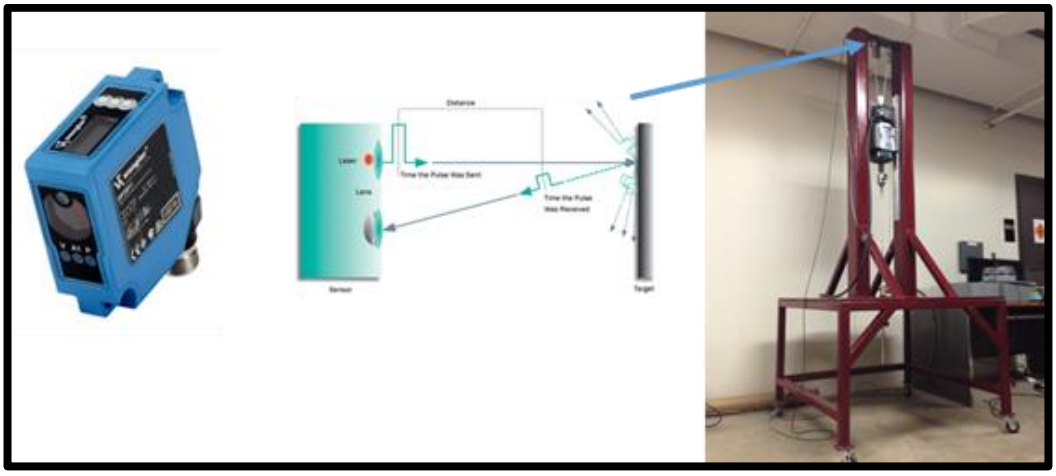

Figure 26: Displacement sensor for ROP and its location on the rig

Downhole Sensors

The downhole sensor will be housed in the BHA to monitor acceleration, inclination, and azimuth. With directionality and the requirement of using downhole data in the control algorithm, this sensor becomes of utmost importance this year. The sensor is shown in figure 27

Fig. 27: Downhole Sensor

Temperature

Temperature measurements are made on the equipment such as the top drive, drawworks motor, hardware interfaces and others to ensure that the equipment is not overloaded. High temperature indicates overload and alarms/ warnings are generated based on the algorithm. A simple RTD, shown in figure 28**,** is sufficient for our system.

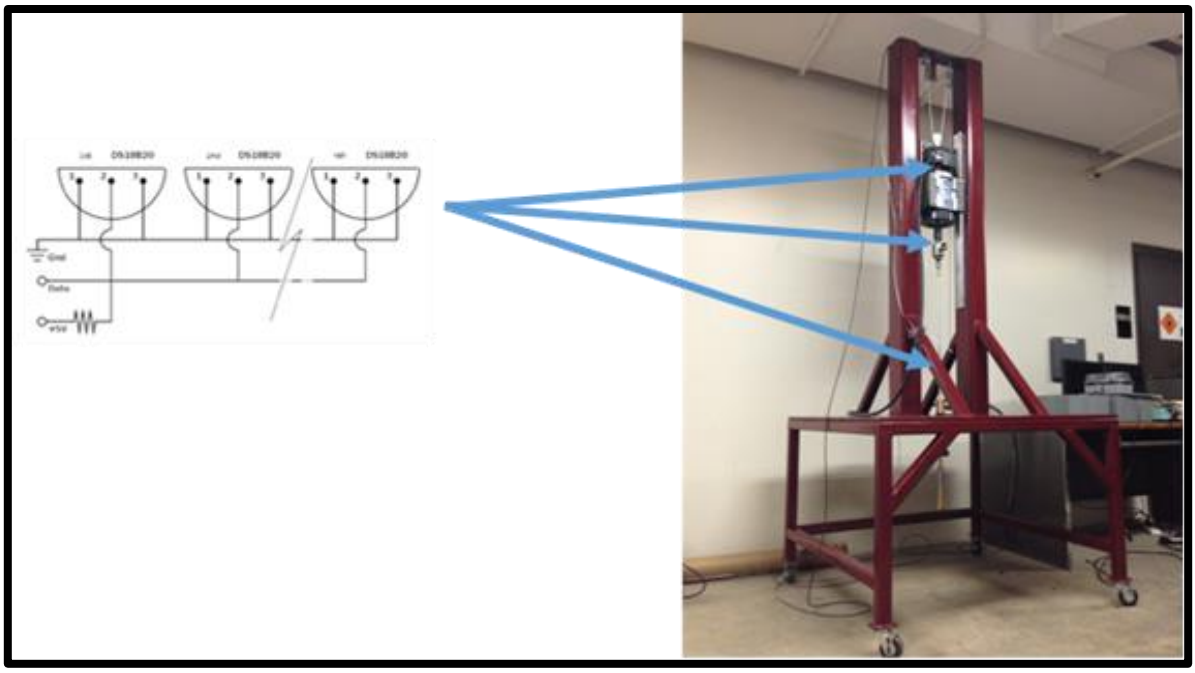

Figure 28: Temperature sensor used and its location on the rig

5.2.2 Data Acquisition

Sensors and transducers measure physical phenomenon such as temperature, tension, pressure, etc. and converts them into a measurable electrical signal like voltage, current, etc. These signals are transferred to a computer by means of a Data Acquisition (DAQ) device. A DAQ device contains several components such as Analog-Digital Converter (ADC, to manipulate the signal to a form readable by computer), Signal Conditioner (to filter out noise and amplify the signal if required), and a Bus (computer bus which is the communication interface).

There are several commercial DAQ devices that are available in the market. Each sensor (or each measurement) requires a DAQ system to transfer the signals to computer and each actuator requires DAQ to receive signals from the computer. We're utilizing a National Instruments DAQ system, as there are several advantages of using NI DAQ devices:

1. Rugged design, accurate measurements with integrated signal conditioning.
2. A single instrument can interpret measurements from various sensors.
3. Multiple timing engines so that data rates from multiple systems are not a problem.
4. LabVIEW for better data handling and data visualization.

We are using NI CompactDAQ 2-slot Chassis (Model number: NI cDAQ-9174) along with Universal Analog Input 4 Ch Module (NI 9219) for the Data Acquisition Purposes. These components are shown in figure 29

Figure 29: Data acquisition modules

In addition to the NI Daq system, we'll be using several standalone data loggers and high speed micro controllers to improve our closed loop response time. We'll be using Arduino Due for high speed requirements and Arduino Uno for non-time sensitive controllers. They have been proven useful for many high speed applications as well as cheap and easily replaceable. Lastly, because of the ease of use and low-overhead cost, we can use several non-critical sensors without running out of inputs/outputs.

6. DATA ANALYTICS

In previous years, optimizing the control system for different lithology was one of the major focuses of the team. The drilling state classifier was an objective, implementing machine learning to identify the lithology being drilled through at a given time. This was done to optimize RPM and WOB so the drilling process would function optimally. We would still like to implement this, but our main focus is to achieve accurate directional drilling. Classifying lithology would not help in the competition due to the sample being homogenous sandstone, but it could help future teams. Our first focus is a high quality wellbore with a correct trajectory.

6.1 Control Architecture, Data Collection and instrumentation

Fundamentally, drilling automation is the control of drilling processes via computer instead of humans. Therefore, designing control system for the processes is key in automation. For automatic control of the rig, we have designed a few control systems in this application. Proportional integral derivative (PID) Controllers will be utilized for rate of penetration (ROP). ROP depends on several factors such as weight on bit (WOB), motor revolutions per minutes (RPM), bit aggressiveness and rock strength among other non-linear effects. The algorithm is developed based on the concept of mechanical specific energy (MSE). MSE concept has been widely used to quantify the efficiency of the energy used to remove the volume of rocks in drilling operation.

ROP control algorithm is designed to minimize MSE and thus improve ROP. New stand-alone motors controllers will be used to accurately control the response for a given reference input. We'll be using two Arduino Due which runs at 84 MHz as a discrete stand-alone controller for certain rig's element, e.g. speed controller's reference followers and high-speed data loggers. Initially, we recorded and analyzed the top drive and drawworks motors transfer function using a black box approach, which analyzes input and output signals and models their frequency response, in addition to trying to model their proper differential equations. The parameters are adjusted as long as the MSE value decreases or remains constant. The ROP should increase proportionately to increase in WOB and RPM. If the increase is not proportionate, it is an indication that the bit is performing inefficiently and that a dysfunction is present in the system.

Sensors and transducers measure physical phenomenon such as temperature, tension, pressure, etc. and converts them into a measurable electrical signal like voltage, current, etc. These signals are transferred into a computer by means of a Data Acquisition (DAQ) device. A DAQ device contains several components such as Analog-Digital Converter (ADC, to manipulate the signal to a form readable by computer), Signal Conditioner (to filter out noise and amplify the signal if required), and a Bus (computer bus which is the communication interface). In addition to the NI Data system, we will be using several standalone data loggers and high speed micro controllers to improve our closed loop response time. We will be using Arduino Due for high speed requirements and Arduino Uno for non-time sensitive controllers. They have been proven useful for many high speed applications as well as cheap and easily replaceable.

6.2 Optimizing Parameters

The parameters that will be controlled are RPM and WOB. In a sample with varying lithology, these would be altered for different rock strengths. The sample this year will have one single compressive strength, but we would expect inclination to cause us to change parameters.
While drilling vertical part, lateral vibration is expected. This is why it is recommended to start drilling with high WOB and less RPM. Then we are going to increase RPM gradually and monitor MSE reading. Then based on MSE reading we are going to optimize drilling parameters On the other hand, when well inclination increase and in horizontal section, weight transfer and stick-slip vibration are expected to be the main challenges. We intended to use maximum RPM and WOB to achieve maximum Rop. Besides that, MSE and torque reading will be monitored to detect any wasted energy or severe vibration encountered. Based on these readings, we are expecting to increase RPM and sometimes decrease WOB to damp stick-slip vibration, ensure effective WOB transfer to bottom better Rop, and effective hole cleaning in horizontal section.

6.3 Control Improvements

As drilling proceeds, several dysfunctions (bit and non-bit) can limit the bit's performance and ultimately hinder the quality of the borehole and the rate of penetration. These dysfunctions are mitigated either by engineering redesign or by adjusting the drilling parameters. The algorithm is developed for real-time corrective action using drilling parameters based on MSE curve response. The objective of the algorithm is to minimize MSE and thus optimize Rate of Penetration (ROP). We have learned the importance of accurately and constantly measuring vibrations through all the procedure. Thus, improving the controller close loop time and delay is of great importance for this phase.

Several steps are taken into consideration, new stand-alone motors controllers will be used to accurately control the response for a given reference input. We'll be using Arduino Due which runs at 84 MHz as a discrete stand-alone controller for certain rig's element, e.g. speed controller's reference followers and high-speed data loggers.

Initially, we recorded and analyzed the top drive and drawworks' motors transfer function using a "black box" approach, which analyzes input and output signals and models their frequency response, in addition to trying to model their proper differential equations. This approach will allow us to properly simulate and develop an accurate and reliable digital controller.

As well as monitoring MSE and adjusting WOB and RPM accordingly, a data-based LQG (Linear Quadratic Gaussian) control loop will also be used to correct trajectory to achieve our target zone, shown in Figure 30. Wc get the Markov parameters from the collected data, and then use these Markov parameters to perform a new design in order t o minimize a finite horizon LQG problem. One of the special features of the data-based control technique is its independence upon the order of the system. It is shown that the data-based LQG control problem is equivalent to the model-based LQG control probleni in the sense of optimality. More importantly, it is shown that to implement an optimal controller, data-based control needs less information than model-based

control. The algorithm will activate the actuator to build more if we are not on the correct trajectory. Based on the survey, LQG controller is going to determine the aggressiveness of the tiltness of the bit through the proposed design well planned.

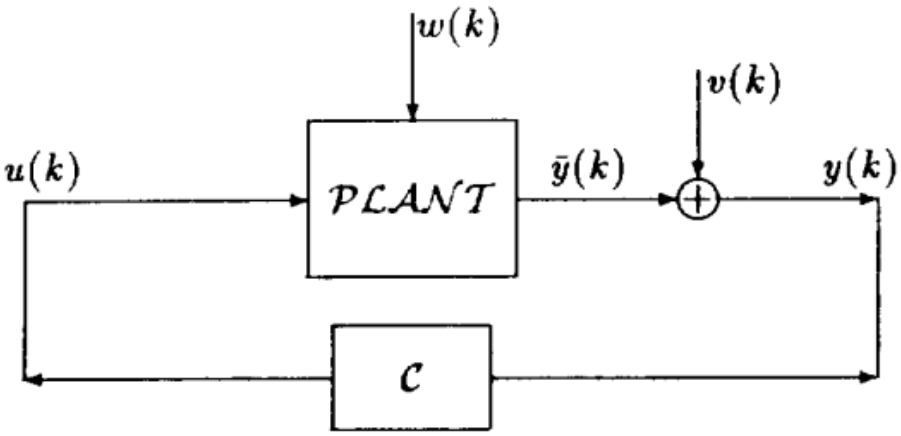

Figure 30 The Data-Based LQG Control Problem

6.4 Auto-Driller Control system

Drilling is carried out automatically using a set WOB. This is achieved by using a scheduled gain PID (Proportional Integral Derivative) Digital Controller developed using the system's dynamic transfer function derived from its analytical differential equations and system identification method. As such, we no longer rely on the "black box" approach. A flow diagram of this process is shown in figure 31**.** Other types of controllers will be considered over the next few months once more data is acquired. Model Predictive Control and Current-Predictors compensators will be tested. Tuning parameters will be done in MATLAB's Simulink.

As discussed, vibration data analytics will be a major component of this control algorithm. A model will be developed to accurately determine the formation type that the system is currently drilling through and applying proper RPM/WOB parameters as a function of the predominant Drill string's vibration frequency and WOB as shown in the flow chart in figure 32

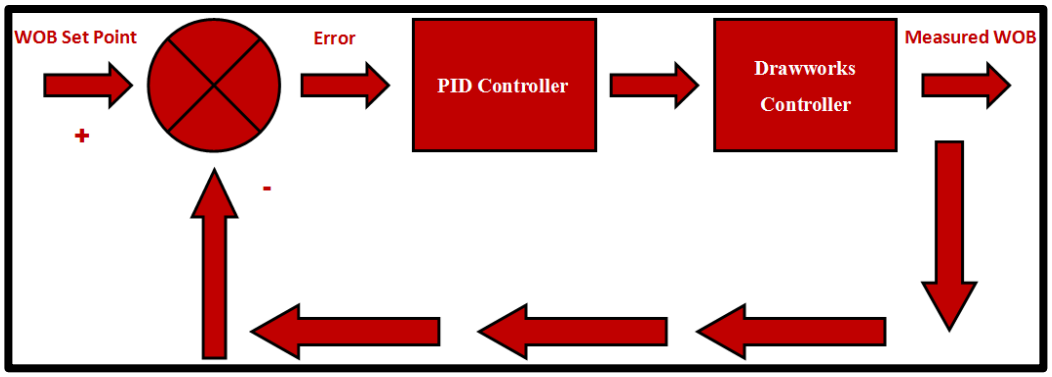

Figure 31: Flow chart depicting Auto-Driller overview

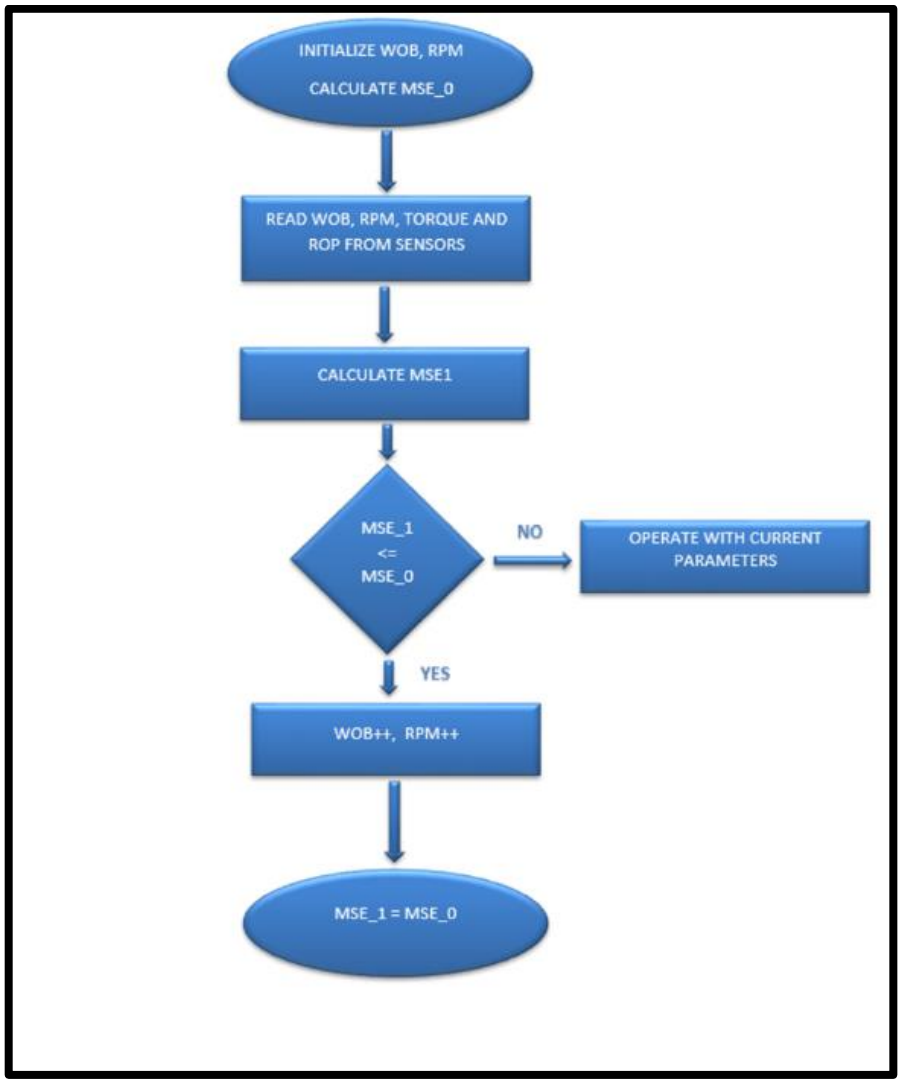

Figure 32: Flow chart depicting the use of MSE to adjust WOB and RPM to maximize ROP

6.5 Data Visualization

LabVIEW has been implemented to develop a simulation environment for experimental purposes. We have chosen LabVIEW for its various advantages such as:

6.4.1 Interactive GUI

A simple, user-friendly interface (called 'Front panel') with graphics can be developed on this platform such that even non-technical people or floor hands can operate.

6.4.2 Hardware integration

NI has powerful data acquisition tools that can acquire data from almost any type of devices. With the help of these tools, it is possible to use the same simulated program developed for mathematical automated models for real-world implementation in the field by simply replacing a few blocks in the program.

6.4.3 Advanced Control

There are several built-in functions (such as PID Auto-tuning, MPC controller among others) in the software, Control Design and Simulation toolkit in particular, which is of high relevance to the drilling automation applications.

The simulation is explained below.

The front panel of the LabVIEW program (called Virtual Instrument or VI) is a user-friendly GUI that depicts the control room at the drilling rig site. Since drilling operations are fully automatic, there are not many parameters for the user to input in the program, other than initialization and motor design parameters to start the simulation.

6.4.4 Data Visualization

The drilling operation (drill bit / string drilling) is displayed as animation and updated in real-time, shown in figure 33. Depth is measured using LVDT is used to update the display. Real-time data is read and transferred to the program. The data is displayed (synchronous with real-time) similarly to those used in the field by the driller. The data includes WOB, Rotary Speed (RPM), Torque and ROP. MSE is calculated using Teale's equation and is displayed along with other parameters. Additionally, azimuth and inclination will be displayed now for directionality.

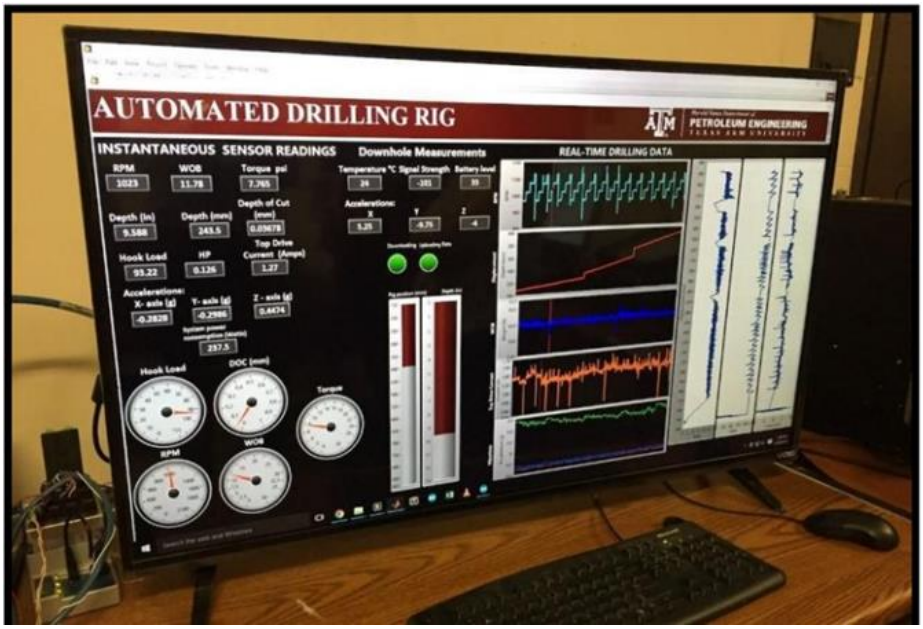

Figure 33: Driller's Display Showing Key parameters in live time

6.4.5 Manual Control

It is important to have manual over-ride controls for all operations that are automated. This is done to ensure control in the case of unpredictable incidents. In the drilling simulator, there are manual controls for adjusting WOB, and RPM, shown in figure 34. We are working on a field-inspired control panel (portable and weatherproof) that will allow the driller to take manual-control over the rig at any point and function like the simulator. An example control panel can be seen in figure 35

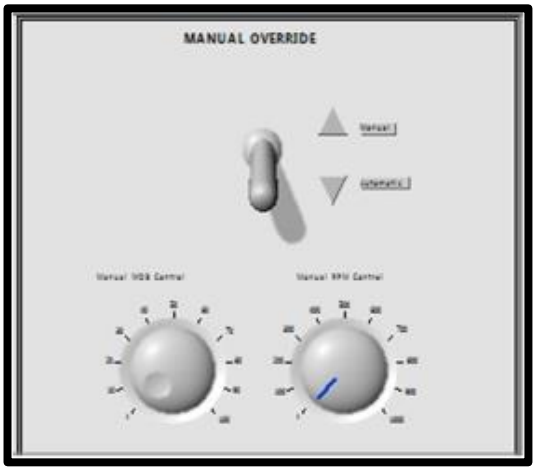

Figure 34: Manual control panel allows for user override at anytime

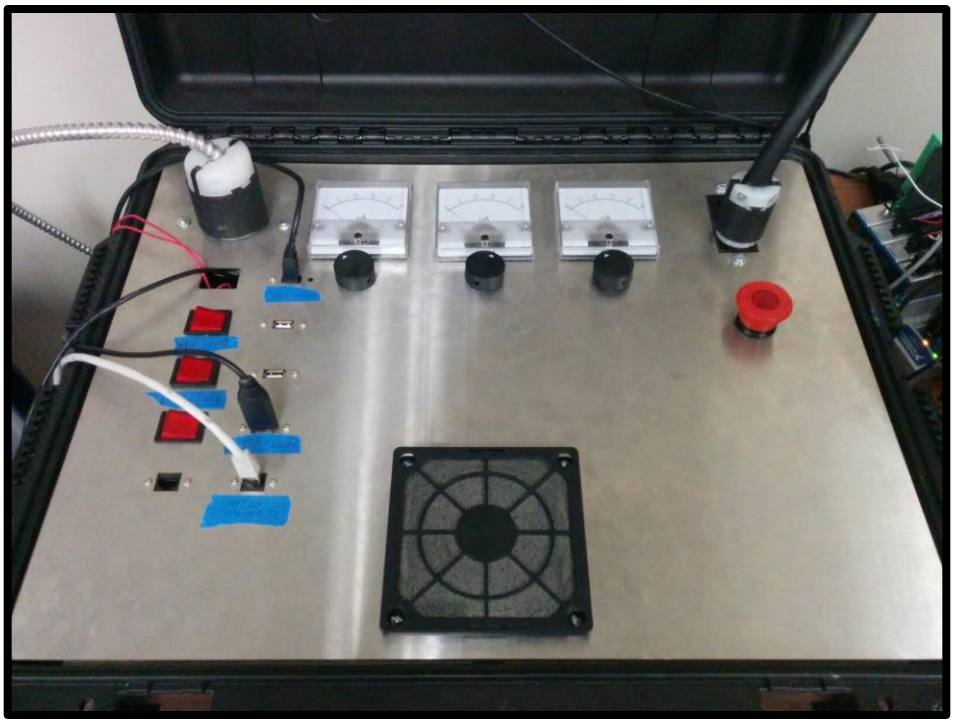

Figure 35: Example control panel

6.4.6 Alarm System

To ensure safe operation, several alarm systems are installed to detect various anomalies.

1. Motor Overload – Drawworks
2. Motor Overload – Top Drive
3. Pump failure
4. Circulation failure
5. Sensor failure

7. Project Plan

The project timeline chart is presented in table 9 Design phase is almost finished and we are expecting to start modifying our test rig at mid of January.

Table 9: Overview of the most common dysfunctions, likelihood of occurrence, and the remedy technique

	Phase	Ocotober				November				December				January				February				March				April			
		1	2	3	4	1	2	3	4	1	2	3	4	1	2	3	4	1	2	3	4	1	2	3	4	1	2	3	4
Rig Construction	Development																												
	Construction & Testing																												
	Integration																												
Drillstring Design	Development																												
	Construction & Testing																												
	Integration																												
Control Architecture & Machine Learning	Development																												
	Construction & Testing																												
	Integration																												
Experimental Phase	Development																												
	Directional Testing (Full Scale)																												

8. Costs Estimates

The following is an estimation of the costs, table 10 associated with updating the rig and its control system. Any unforeseen costs (new ideas, part failures, etc.) that are experienced in the coming months will be addressed in an updated spreadsheet attached to the corresponding monthly report. The majority of the costs are expected to be in acquiring and developing new equipment for directional drilling. The estimates are on the high end.

Table 10 - Cost Estimates

Cost Estimates		
#	Item	Amount, USD
1	New Rig Construction	2000
2	Drill Pipe	375
3	RSS and Bit	1500
4	Electronics	2000
5	Connection and Coupling	200
6	Welding Equipments	200
7	Repairs	700
8	Tools	500
	Total	7475

9. References

1. Skelton, Robert E., and Mauricio C. de Oliveira. Tensegrity systems. Vol. 1. New York: Springer, 2009.

2. Nagase, K., and R. E. Skelton. "Double-helix tensegrity structures." Aiaa Journal 53.4 (2014): 847-862.

3. Teale, R. (1965, March). The concept of specific energy in rock drilling. In International Journal of Rock Mechanics and Mining Sciences & Geomechanics Abstracts (Vol. 2, No. 1, pp. 57–73). Pergamon.